East European Journal of Physics. **4.** 23-47 (2022)
DOI:10.26565/2312-4334-2022-4-02 ISSN 2312-4334

A BIO-THERMAL CONVECTION IN A POROUS MEDIUM SATURATED BY NANOFLUID CONTAINING GYROTACTIC MICROORGANISMS UNDER AN EXTERNAL MAGNETIC FIELD[†]

Michael I. Kopp[a]*, Volodymyr V. Yanovsky[a,b], Ulavathi S. Mahabaleshwar[c]
[a]*Institute for Single Cristals, Nat. Academy of Science Ukraine,*
Nauky Ave. 60, Kharkiv 31001,Ukraine
[b]*V.N. Karazin Kharkiv National University*
4, Svoboda Sq., Kharkiv, 61022, Ukraine
[c]*Department of Mathematics, Shivagangotri, Davangere University, Davangere, India 577 007*
**Corresponding Author: michaelkopp0165@gmail.com*
Received September 23, 2022; revised October 30, 2022; accepted November 3, 2022

The study of thermal convection in porous media saturated by nanofluid and microorganisms is an important problem for many geophysical and engineering applications. The concept of a mixture of nanofluids and microorganisms has attracted the interest of many researchers due to its ability to improve thermal properties and, as a result, heat transfer rates. This property is actively used both in electronic cooling systems and biological applications. Thus, the purpose of this research is to study biothermal instability in a porous medium saturated by a water-based nanofluid containing gyrotactic microorganisms in the presence of a vertical magnetic field. Given the presence of an external magnetic field in both natural and technological situations, we were motivated to perform this theoretical research. Using the Darcy-Brinkman model, a linear analysis of the convective instability has been considered for both-free boundaries, taking into account the effects of Brownian diffusion and thermophoresis. The Galerkin method was used to perform this analytical study. We have established that heat transfer is accomplished by stationary convection without oscillatory movements. In stationary convection regimes, metal oxide nanofluids (Al_2O_3), metallic nanofluids (Cu, Ag), and semiconductor nanofluids (TiO_2, SiO_2) are analyzed. Increasing the Chandrasekhar and Darcy numbers improve system stability significantly, but increasing porosity and modified bioconvection Rayleigh-Darcy number speed up the beginning of instability. To determine the transient behavior of heat and mass transports, a non-linear theory based on the representation of the Fourier series method is applied. In small time intervals, the transitional Nusselt and Sherwood numbers exhibit an oscillatory character. The Sherwood numbers (mass transfer) in the time interval reach stationary values faster than the Nusselt numbers (heat transfer). This research might help with seawater convection in the oceanic crust as well as the construction of biosensors.
Keywords: nanofluid, bio-thermal convection, Lorentz force, thermophoresis, Brownian motion, gyrotactic microorganism, magnetic field
PACS: 44.10.+i, 44.30.+v, 47.20.-k

1. INTRODUCTION

Many theoretical and practical study in fields such as soil mechanics, groundwater hydrology, petroleum engineering, industrial filtration, powder metallurgy, nuclear energy, and so on have been based on the study of the physics of flow through a porous media. Such flows through porous media are of great interest to petroleum engineers and geophysical fluid dynamicists. The problem of thermal instability of a liquid layer in a porous medium is of special importance. Ingham and Pop [1] as well as Nield and Bejan [2] provide excellent reviews of the most of the studies on convection in porous media. The issues of fluid flow and heat transfer in rotating porous media have been studied in detail in a recent review by Vadasz [3].

Objects with dimensions of less than one hundred nanometers have developed as a result of the progress of nanotechnology. Such nanosized objects are called nanoparticles. Choi [4] proposed suspending these nanoparticles in a base fluid (known as nanofluid) to improve heat conductivity and convective heat transfer of the base fluid. Thus, nanofluids began to be intensively used in industry, such as coolants, lubricants, heat exchangers, microchannel radiators, and many others. Buongiorno [5] extensively studied convective transport in nanofluids and concentrated on explaining the additional heat transfer increases observed under convective flows. Tzou [6] used Buongiorno transport equations to study the onset of convection in a horizontal layer uniformly heated from below for a nanofluid and discovered that due to Brownian motion and thermophoresis of nanoparticles, the critical Rayleigh number is much lower, by one to two orders of magnitude, than that of an ordinary fluid.

Because of the remarkable characteristics of nanofluids in heat transfer phenomena, research involving nanofluids in a porous media has become required. Kuznetsov and Nield [7]-[8] used the Brinkman model to investigate the onset of thermal instability in a porous media saturated with a nanofluid, taking into account Brownian motion and nanoparticle thermophoresis. They discovered that the presence of nanoparticles may significantly lower or increase the critical thermal Rayleigh number, depending on whether the basic nanoparticle distribution is top-heavy or bottom-heavy. Further, Bhadauria and Agarwal [9] and Yadav et al. [10] extended the thermal instability problem by including

[†] ***Cite as:*** M.I. Kopp, V.V. Yanovsky, and U.S. Mahabaleshwar, East Eur. J. Phys. **4**, 23 (2022), https://doi.org/10.26565/2312-4334-2022-4-02

the Coriolis force term (rotation) in momentum equations for porous and non-porous materials, concluding that including the Coriolis force component made the overall system more stable. Bhadauria and Agarwal [9] made a nonlinear investigation of nanofluid convection in a rotating porous layer in terms of Nusselt number. Chand and Rana [11] used the Darcy-Brinkman model to investigate the influence of rotation on nanofluid convection. For stationary convection, an equation for the thermal Rayleigh number was found. Gupta et al. [12] studied the onset of convection in a horizontal nanofluid layer in the presence of a vertical magnetic field and discovered that stability increases as the magnetic field value increases. The effects of a magnetic field on a horizontal layer of nanofluid have several significant characteristics, making it necessary to explore the effects of a magnetic field in a porous medium. Ahuja et al. [13] used the Darcy-Brinkman model to explore the thermal convection of a nanofluid layer in the presence of an applied vertical magnetic field saturated by a porous medium for both-free, rigid-free, and both-rigid barriers. The effect of an externally applied magnetic field on the stability of a binary nanofluid layer in porous medium is considered by Sharma et al. [14]. It was established that semiconducting nanofluids are found to be more stable than metallic nanofluids. Furthermore, porosity destabilizes the layer while solute difference (at the boundaries of the layer) stabilizes it and the magnetic field stabilizes the fluid layer system significantly. Yadav et al. [15] investigated the effect of Hall current on the criterion for the onset of MHD convection in a porous medium layer saturated by a nanofluid. They were shown that the increase in the Hall current parameter, the Lewis number, the modified diffusivity ratio, and the concentration Rayleigh Darcy number is to hasten the onset of convection while the magnetic Darcy number, the porosity parameter and the Darcy number have stabilized on the onset of convection. Ahuja and Gupta [16] investigated the onset of thermal convection of a porous nanofluid layer under the combined influence of rotation and magnetic field using the Darcy-Brinkman model. As shown in[16], the stability of the system enhances with the rise in Chandrasekhar number and Taylor number whereas it falls with the rise in porosity. According to [16] silver nanoparticles stabilized water-based fluids better than copper nanoparticles, while TiO_2 nanoparticles in semiconductors improve system stability better than SiO_2 nanoparticles.

A detailed review of the current state of the problem of MHD convection in nanofluids presents in [17]. The article [18] discusses a new review devoted to the subject of Rayleigh-Benard instability in a nanofluid. In addition to the above, a relatively new area of research: bioconvection inside a nanofluid is of great importance in applied problems of creating biosensors, microdevices for measuring the toxicity of nanoparticles. Bioconvection is the movement of a fluid medium caused by a directed flow of microorganisms that results in a redistribution of the medium's density. As a result, hydrodynamic processes in the medium emerge, analogous to natural convection in the presence of temperature gradients. Bioconvection takes into account the movement of bacteria and algae, with microorganisms having a higher density than water. Microorganisms can move due to gravity forces (gyrotactic microorganisms), oxygen concentration gradients (oxytactic microorganisms), light radiation (phototaxis microorganisms), nutrition gradients (chemotaxis microorganisms), and other factors. The number of self-propelled microorganisms can be quite considerable, varying from 10^7 cm^{-3} in a low concentratin regime to 10^{11} cm^{-3} in a turbulent regime with almost densely packed microorganisms. A linear theory of the stability of bioconvection of gyrotactic microorganisms in a finite depth layer of an ordinary fluid was developed by Pedley et al. [19]-[21]. In these works, the criteria for the onset of a bioconvective flow were determined. Avramenko [22] based on the Lorenz approach [23] a nonlinear theory of bioconvection for gyrotactic microorganisms in a layer of ordinary liquid was developed. In [22], the boundaries of various hydrodynamic regimes of two-dimensional bioinvection were determined.

Unlike microorganisms, nanoparticles are not self-propelled, move due to Brownian motion and thermophoresis, and are driven by fluid flow. Kuznetsov's [24],[25] works are devoted to the interaction of nanofluids with bioconvection. The paper [24] investigated the possibility of oscillatory instability in a nanofluid suspension containing oxitate bacteria. In [25] analyzes the combined influence on the onset of biothermal convection in suspension, nanoparticles, gyrostatic microorganisms, and algae. A linear analysis of the instability is performed, allowing the bounds of the oscillatory instability to be determined. The destabilizing effect of Brownian motion and thermophoresis of nanoparticles, vertical throughflow, and gyrotactic microorganisms on biothermal instability was discovered by Saini and Sharma [26].

Because of the practical nature of the problem, a significant number of works (for example, [27-31]) have recently arisen that investigate two-dimensional magnetohydrodynamic flows and the processes of heat and mass transfer of a watery nanofluid, including gyrotactic microorganisms. The effects of buoyancy, Brownian motion, thermophoresis, and chemical reactivity on bioconvection of nanofluidic gyrostatic microorganisms are investigated in these papers. The aim of using microorganisms is to stabilize nanoparticle suspensions created by bioconvection caused by the combined effects of buoyancy and magnetic field forces.

There are a lot of publications on the effect of gyrotactic microorganisms on nanofluid flows in bounded porous media. The study of biological processes in porous media has recently rapidly progressed. Kuznetsov, Nield, and Avramenko [32-36] made a significant contribution to the dynamics of biological processes in porous media. A linear analysis of biothermal convection based on the Darcy-Brinkman model in a suspension of gyrotactic microorganisms in a highly porous medium heated from below was carried out in [37]. The following conclusions [37] were drawn there: a suspension containing faster-swimming cells is more unstable; gyrotaxis contributes to the development of bioconvection instability; the modified Darcy number associated with the effective viscosity stabilizes the slurry.

Recently, the flow of boundary layers of natural convection nanofluids over a vertical flat plate embedded in a saturated porous Darcy medium containing gyrotactic microorganisms was studied in studies[38]-[40]. The effects of dimensionless parameters, such as the Lewis number of bioconvection, the Rayleigh number of bioconvection, the Peclet number of bioconvection, the Brownian motion parameter, the buoyancy coefficient, the thermophoresis parameter, the index of change of the power law, and the Lewis number, on the flow characteristics of the bioconvection process are analyzed during a numerical solution.

Despite significant progress in the study of bioconvection in porous media, the impact of gyrotactic organisms on thermal instability in a layer of a porous media saturated by a nanofluid under the action of a magnetic field has yet to be investigated. Of particular interest is the study of the linear and nonlinear stages of bio-thermal convection in a porous medium saturated with nanofluid for various types of nanoparticles such as metal, metal oxides, and semiconductor nanoparticles under an external magnetic field. The aim of this paper is to investigate the abovementioned problem.

The content of the paper is presented in the following sections. The Introduction (section 1) presents a review of the literature on this issue. In section 2, we describe the problem statement and obtain evolution equations in the Boussinesq-Oberbeck approximation in a layer of a Darcy-Brinkman porous medium saturated by an electrically conducting nanofluid with gyrotactic microorganisms. In section 3, we obtained equations for the basic state and small perturbations in dimensionless form. The equation for the vertical component of the perturbed velocity was obtained using the elimination of variables technique. This equation is supplemented with conditions for free-free boundaries. In section 4, we derive a general dispersion equation taking into account the effects of a vertical magnetic field, gyrotactic microorganism bioconvection, Brownian diffusion of nanoparticles, and thermophoresis. The oscillatory and stationary regimes of mixed convection are considered. In section 5, we study the non-linear theory based on the representation of the Fourier series method used to find the temporary behavior of heat and mass transports. In section 6, we analyze the linear regime of stationary convection and calculate the expressions for heat and mass transports. In section 7, we perform a numerical/graphical analysis of the development of stationary convection carried out for oxide metal, metallic, and semiconductor nanofluids. Convective heat and mass transfers in terms of Nusselt number $Nu(t)$ and Sherwood number $Sh(t)$ were calculated. The Conclusions present the main conclusions of this paper.

2. STATEMENT OF THE PROBLEM AND BASIC EQUATIONS

Let us consider an infinite horizontal layer of incompressible electrically conductive nanofluid containing nanoparticles and gyrotactic microorganisms in a homogenous porous medium. Initially, a homogeneous porous layer with a thickness of h is assumed to be at rest. Heating from below the layer causes disturbance, where T_d, T_u are the temperatures and ϕ_d, ϕ_u $(\phi_u > \phi_d)$ are the volume fractions of nanoparticles at the lower and upper boundaries, respectively (as shown in Fig. 1). The presence of nanoparticles is considered to not affect the direction and speed with which microorganisms swim. Physically, this is possible if a flow generated by bioconvection exists for a small concentration of nanoparticles. The terminology for nanoparticles are written using Buongiorno's [5] theory, whereas those for gyrotactic microorganisms are written using Pedley's [19]-[21] approach.

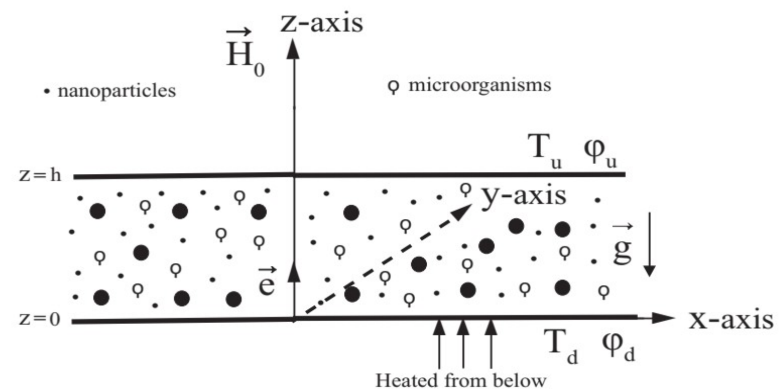

Figure 1. Geometry and coordinate system of the problem

Fig. 1 depicts the problem's geometry. We used the Cartesian coordinates (x, y, z) with the z-axis points vertically upward. The gravitational force $\vec{g} = (0, 0, -g)$ acts vertically downwards, while the magnetic field $\vec{H}_0 = (0, 0, H_0)$ acts vertically upwards. $\vec{V}_D$ is the Darcy velocity, which is related to the nanofluid velocity $\vec{V}$ as $\vec{V}_D = \varepsilon \vec{V}$. The physical model of our problem consists of the following assumptions:

• All thermophysical characteristics are constant except for density in the buoyant force (Boussinesq approximation).

• Because the fluid phase, microorganisms, and nanoparticles are in a condition of thermal equilibrium, the heat flow may be described using a one equation model.

• Nanofluid is incompressible, electrically conducting, viscous, laminar, and nanoparticles are non-magnetic spherical particles.

• Each boundary wall is assumed to be impermeable and perfectly thermal conducting.

• The porous material is completely saturated with a nanofluid in which microorganisms can swim.

• The material's pores must be big enough to accommodate biological organisms and their movement.

• The solid porous matrix does not absorb microorganisms, and each one has the same volume and form, as well as swimming at the same speed.

• The heating from below has no influence on the cells' gyrotactic activity and does not kill them.

According to the above assumptions, the bioconvective motion of gyrotactic microorganisms in a porous medium saturated with nanofluid in the presence of a magnetic field will be described using the Darcy-Brinkman model. Let's suppose that a suspension of swimming microorganisms and nanoparticles is incompressible, and therefore

$$\nabla\cdot \vec{V}_D = 0, \tag{1}$$

The conservation equation for the nanoparticles given by

$$\frac{\partial \phi}{\partial t}+\left(\frac{\vec{V}_D}{\varepsilon}\cdot \nabla\right)\phi = D_B\nabla^2\phi+\frac{D_T}{T_u}\nabla^2 T, \tag{2}$$

The conservation equation of cells is given by [20, 32,33]

$$\frac{\partial n}{\partial t}=-div\left(n\vec{V}_D+nW_c l-D_m\nabla n\right), \tag{3}$$

The momentum equation can be written using the Boussinesq approximation [7] as

$$\frac{\rho_0}{\varepsilon}\frac{\partial \vec{V}_D}{\partial t}=-\nabla P+\tilde{\mu}\nabla^2\vec{V}_D-\frac{\mu}{K}\vec{V}_D+\frac{\mu_e}{4\pi}(\vec{H}\cdot \nabla)\vec{H}+\vec{g}[\phi\rho_p+(1-\phi)\rho_0(1-\beta(T-T_u))]+\vec{g}(\delta\rho)\mathcal{V}n \tag{4}$$

here the buoyancy force is made up of three different components: the fluid's temperature change, the distribution of nanoparticles (nanoparticles are heavier than water), and the concentration of microorganisms (microorganisms are also heavier than water). In equation (4), the external magnetic field is taken into account with the help of an additional force, the Lorentz force, which affects the movement of the electrically conductive nanofluid.

The thermal energy conservation equation is

$$(\rho c)_m\frac{\partial T}{\partial t}+(\rho c)_f\vec{V}_D\cdot \nabla T = k_m\nabla^2 T+\varepsilon(\rho c)_p\left(D_B\nabla\phi\cdot \nabla T+D_T\frac{\nabla T\cdot \nabla T}{T_1}\right) \tag{5}$$

The inductive magnetic fields caused by convective flows of an electrically conductive nanofluid is described by the following equations [41]

$$\frac{\partial H}{\partial t}+\left(\frac{V_D}{\varepsilon}\cdot \nabla\right)H=\left(H\nabla\right)\frac{V_D}{\varepsilon}+\eta\nabla^2 H \tag{6}$$

$$\nabla\cdot \vec{H}=0\,, \tag{7}$$

here $\rho=\phi\rho_p+(1-\phi)\rho_f$ is the nanofluid density, $\rho_0=\phi\rho_p+(1-\phi)\rho_{f0}$ is the nanofluid reference density, ρ_p and ρ_f are the density of nanoparticle and base fluid, respectively. ρ_{f0} is the base fluid density at the reference temperature T_u, ϕ is the volumetric fraction of nanoparticles. D_B and D_T denote the Brownian diffusion coefficient and thermophoretic diffusion, respectively. $(\rho c)_f,(\rho c)_p,(\rho c)_m$ are fluid heat capacity, nanoparticles heat capacity and medium heat capacity, respectively. n is the concentration of microorganisms, $\delta\rho$ is the density difference between microorganisms and a base fluid: $\rho_m-\rho_f$, $\mathcal{V}$ is the average volume of a microorganism, D_m is the diffusivity of microorganisms. We assumed that random motions of microorganisms are simulated by a diffusion process. $W_c\vec{l}$ is the average microorganism swimming velocity (W_c is constant, $\vec{l}$ is a unit vector of movement of microorganisms). P is the pressure, β is the thermal expansion coefficient, $\vec{e}=(0,0,1)$ is a unit vector in the direction of the axis z. ε is the porosity of the porous medium, K is the permeability of the porous medium, $\tilde{\mu}$ is the effective viscosity, μ, η and μ_e are the viscosity, magnetic viscosity and magnetic permeability of nanofluid, respectively.

We assume that the temperature and volume fraction of nanoparticles have fixed values at the boundaries of the porous layer.

$$w=0,\quad T=T_d,\quad \phi=\phi_d,\quad \vec{J}\cdot\vec{e}=0,\quad at\quad z=0 \tag{8}$$

$$w=0,\quad T=T_u,\quad \phi=\phi_u,\quad \vec{J}\cdot\vec{e}=0,\quad at\quad z=h, \tag{9}$$

where $\vec{J}=n\dfrac{\vec{V}_D}{\varepsilon}+nW_c\vec{l}-D_m\nabla n$ is the flux of microorganisms.

Let us introduce the following non-dimensional parameters

$$(x^*,y^*,z^*)=\frac{(x,y,z)}{h},\vec{V}_D^*(u^*,v^*,w^*)=\vec{V}_D(u,v,w)\frac{h}{\alpha_m},t^*=\frac{t\alpha_m}{h^2\tilde{\sigma}},$$

$$P^*=\frac{PK}{\mu\alpha_m},\quad \alpha_m=\frac{k_m}{(\rho c)_f},\quad \tilde{\sigma}=\frac{(\rho c)_m}{(\rho c)_f},\quad n^*=\frac{n}{N_0}, \tag{10}$$

$$\vec{H}^*=\frac{\vec{H}}{H_0},\quad \phi^*=\frac{\phi-\phi_d}{\phi_u-\phi_d},\quad T^*=\frac{T-T_u}{T_d-T_u},$$

where $N_0=const$ is average concentration of microorganisms in the layer. Using expressions (10) and omitting the asterisks, we get the following system of dimensionless equations

$$\nabla\cdot\vec{V}_D=0, \tag{11}$$

$$\frac{1}{\tilde{\sigma}}\frac{\partial\phi}{\partial t}+\left(\frac{\vec{V}_D}{\varepsilon}\cdot\nabla\right)\phi=\frac{1}{L_e}\nabla^2\phi+\frac{N_A}{L_e}\nabla^2T, \tag{12}$$

$$\frac{1}{\sigma}\frac{\partial n}{\partial t}=-\nabla\left(n\vec{V}_D+\frac{Pe}{L_b}n\vec{l}-\frac{1}{L_b}\nabla n\right), \tag{13}$$

$$\begin{aligned}\frac{1}{\mathcal{V}_a}\frac{\partial\vec{V}_D}{\partial t}&=-\nabla P+D_a\nabla^2\vec{V}_D-\vec{V}_D-\vec{e}R_m-\vec{e}R_n\phi-\vec{e}\frac{R_b}{L_b}N+\\&+\vec{e}RaT+Q\frac{Pr}{Pm}(\vec{H}\cdot\nabla)\vec{H}\end{aligned}, \tag{14}$$

$$\frac{\partial T}{\partial t}+(\vec{V}_D\nabla)T=\nabla^2T+\frac{N_B}{L_e}\nabla\phi\cdot\nabla T+\frac{N_AN_B}{L_e}(\nabla T)^2, \tag{15}$$

$$\frac{1}{\tilde{\sigma}}\frac{\partial\vec{H}}{\partial t}+\left(\frac{\vec{V}_D}{\varepsilon}\cdot\nabla\right)\vec{H}=(\vec{H}\cdot\nabla)\frac{\vec{V}_D}{\varepsilon}+\frac{Pr}{Pm}\nabla^2\vec{H}, \tag{16}$$

$$\nabla\cdot\vec{H}=0. \tag{17}$$

In Eqs. (11)-(17), we introduced the following dimensionless parameters:

$\mathcal{V}_a=\dfrac{\varepsilon Pr}{D_a}\dfrac{\tilde{\mu}(\rho c)_m}{\mu(\rho c)_f}$ is the modified Vadasz number, $D_a=\dfrac{\tilde{\mu}K}{\mu h^2}$ is the Darcy number, $Pr=\dfrac{\mu}{\rho_0\alpha_m}$ is the Prantdl number, $Pm=\dfrac{\mu}{\rho_0\eta}$ is the magnetic Prantdl number, $L_e=\dfrac{\alpha_m}{D_B}$ is the nanoparticle Lewis number, $L_b=\dfrac{\alpha_m}{D_m}$ is the bioconvection Lewis number, $Q=\frac{\mu_e H_0^2 K}{4\pi\mu\eta}$ is the Chandrasekhar-Darcy number, $R_b=\frac{ghN_0(\delta\rho)VK}{\mu D_m}$ is the bioconvection Rayleigh-Darcy number, $R_m=\frac{[\rho_p\phi_d+\rho_0(1-\phi_d)](ghK)}{\mu\alpha_m}$ is the basic density Rayleigh-Darcy number, $R_n=\frac{(\rho_p-\rho_0)(\phi_u-\phi_d)ghK}{\mu\alpha_m}$ is the concentration Rayleigh-Darcy number, $Ra=\frac{\rho_0 ghK\beta(T_d-T_u)}{\mu\alpha_m}$ is the Rayleigh-Darcy number, $N_B=\frac{\varepsilon(\rho c)_p}{(\rho c)_f}(\phi_u-\phi_d)$ is the modified nanoparticles density, $N_A=\frac{D_T(T_d-T_u)}{D_B T_u(\phi_u-\phi_d)}$ is the modified diffusivity ratio, $Pe=\frac{W_c h}{D_m}$ is bioconvection Peclet number.

Eq. (14) has been linearized using a small temperature gradient in a dilute suspension of nanoparticles and microorganisms using the Boussinesq approximation. Equations (11)-(17) are supplemented with boundary conditions in non-dimensional form:

$$w=0,\quad T=1,\quad \phi=0,\quad Pen=\frac{dn}{dz},\quad at\ z=0, \tag{18}$$

$$w=0,\quad T=0,\quad \phi=1,\quad Pen=\frac{dn}{dz},\quad at\ z=1. \tag{19}$$

2. EQUATIONS FOR PERTURBATIONS

Let's start with the assumption that the fluid layer is at rest. The physical system is then moved slightly out of its equilibrium position. We assume that all variables in Eqs. (11)-(17) can describe the sum of the steady and perturbed components:

$$V_b=0,\quad P=P_b(z)+p',\quad T=T_b(z)+T',\quad \phi=\phi_b(z)+\phi',\quad n=n_b(z)+n',\quad \vec{l}=\vec{e}+\hat{\vec{m}}'. \tag{20}$$

The steady profiles of temperature $T_b(z)$ and the volume fraction of nanoparticles $\phi_b(z)$ are found from the solutions of the equations

$$\frac{d^2T_b}{dz^2}+\frac{N_B}{L_e}\frac{d\phi_b}{dz}\frac{dT_b}{dz}+\frac{N_A N_B}{L_e}\left(\frac{dT_b}{dz}\right)^2=0, \tag{21}$$

$$\frac{d^2\phi_b}{dz^2}+N_A\frac{d^2T_b}{dz^2}=0.$$

Taking into account the experimental data for most nanofluids [5], a good approximation of the base state (21) is a linear dependence on z for $T_b(z)$ and $\varphi_b(z)$ (see, for example, [16]):

$$T_b(z)=1-z,\quad \phi_b(z)=z. \tag{22}$$

The pressure distribution in the ground state satisfies the equation

$$\frac{dP_b(z)}{dz}=-R_m-R_n\phi_b(z)-\frac{R_b}{L_b}N_b(z)+RaT_b(z), \tag{23}$$

from which the explicit form $P_b(z)$ may be found by integration. The stationary profile of the concentration of microorganisms $n_b(z)$ is determined by the following expression [19]

$$n_b(z)=N_0\cdot\frac{Pe\exp(zPe)}{\exp(Pe)-1}, \tag{24}$$

For the case of small Peclet numbers Pe, it follows from (24) that $n(z)\approx N_0=const$. Following the approach as in article [22], to simplify the, we will focus on this case.

According to publications[19],[analysis 32], the equation for the perturbation of a unit vector indicating the direction of swimming of microorganisms has the following form:

$$\hat{\vec{m}}' = \mathcal{B}\zeta\vec{i} - \mathcal{B}\xi\vec{j} + 0\cdot\vec{e}, \tag{25}$$

where $\vec{i}$ and $\vec{j}$ are the unit vectors in the x- and y-directions, respectively. $\mathcal{B} = (3\tilde{\mu}/\rho_m g d)(\alpha_m / h^2)$ is a dimensionless parameter characterizing the reorientation of microorganisms under the action of a gravitational moment against viscous resistance, d is the displacement of the center of mass of the cell from the center of buoyancy. In Eq. (25), the parameters ζ and ξ in the x- and y-components of vector $\hat{\vec{m}}'$ are

$$\zeta = -(1-\alpha_0)\frac{\partial w'}{\partial x} + (1+\alpha_0)\frac{\partial u'}{\partial z}, \tag{26}$$

$$\xi = (1-\alpha_0)\frac{\partial w'}{\partial y} - (1+\alpha_0)\frac{\partial v'}{\partial z}.$$

α_0 is the cell eccentricity which is given by the following equation [19,32]:

$$\alpha_0 = \frac{r_{max}^2 - r_{min}^2}{r_{max}^2 + r_{min}^2}, \tag{27}$$

where r_{max} and r_{min} are the semi-major and semi-minor axes of the spheroidal cell.

Taking into account Eqs. (25)-(26), we get the following equation for the perturbation of the cell number density:

$$\frac{1}{\tilde{\sigma}}\frac{\partial n'}{\partial t} + \frac{Pe}{L_b}\frac{dn'}{dz} - PeG\left((1+\alpha_0)\frac{d^2 w'}{dz^2} + (1-\alpha_0)\left(\frac{\partial^2 w'}{\partial x^2} + \frac{\partial^2 w'}{\partial y^2}\right)\right) = \frac{1}{L_b}\nabla^2 n', \tag{28}$$

where $G = D_m\mathcal{B}/h^2$ is a dimensionless orientation parameter [22].

After substituting (20) into the equations (12)-(16), we get equations for the variables $u', v', w', T', \phi', b'$, which are also linearized. Further, the analysis of equations for the perturbation will be investigated by the method of normal modes, assuming that the perturbing quantities have the following form:

$$[u', v', w', T', \phi', n', b'] = [U(z), V(z), W(z), \Theta(z), \Phi(z), N(z), B(z)]e^{i(k_x x + k_y y + \gamma t)}, \tag{29}$$

where k_x, k_y are the wave number along the x and y directions, and $a = \sqrt{k_x^2 + k_y^2}$ is the horizontal wave number of the disturbances. The growth rate parameter is denoted by γ.

Using (29), we get the linearized equations in dimensionless form after a few simple but cumbersome transformations:

$$\left(D_a(D^2-a^2) - \frac{\gamma}{V_a} - 1\right)(D^2-a^2)W - a^2 Ra\Theta + a^2 R_n\Phi + \frac{a^2 R_b}{L_b}N + \frac{QPr}{Pm}D(D^2-a^2)B_z = 0, \tag{30}$$

$$\left(D^2 - a^2 - \gamma + \frac{N_B}{L_e}(1-2N_A)D\right)\Theta - \frac{N_B}{L_e}D\Phi + W = 0, \tag{31}$$

$$\left(D^2 - a^2 - \frac{\gamma L_e}{\tilde{\sigma}}\right)\Phi + N_A(D^2-a^2)\Theta - \frac{L_e W}{\varepsilon} = 0, \tag{32}$$

$$\left(\frac{1}{L_b}(D^2-a^2) - \frac{Pe}{L_b}D - \frac{\gamma}{\tilde{\sigma}}\right)N + PeG((1+\alpha_0)D^2 - (1-\alpha_0)a^2)W = 0, \tag{33}$$

$$\left(\frac{Pr}{Pm}(D^2-a^2) - \frac{\gamma}{\tilde{\sigma}}\right)B_z + \frac{DW}{\varepsilon} = 0. \tag{34}$$

The system of equations (30)-(34) is reduced to one equation for W using the elimination of variables technique

$$\left[\begin{array}{l}\hat{L}\hat{L}_D\hat{L}_\phi\hat{L}_B\hat{L}_N\left(D^2-a^2\right)+a^2Ra\hat{L}_\phi\hat{L}_B\hat{L}_N\left(\hat{L}_\phi-\dfrac{N_B}{\varepsilon}D\right)+\\ +a^2R_n\hat{L}_B\hat{L}_N\left(\hat{L}\dfrac{L_e}{\varepsilon}+N_A(D^2-a^2)\left(\hat{L}_\phi-\dfrac{N_B}{\varepsilon}D\right)\right)-\\ -a^2\dfrac{R_b}{L_b}\alpha\hat{L}\hat{L}_\phi\hat{L}_B-\dfrac{QPr}{\varepsilon Pm}\hat{L}\hat{L}_\phi\hat{L}_N D^2\left(D^2-a^2\right)\end{array}\right]W=0, \tag{35}$$

where the operators are

$$\hat{L}=\hat{L}_T\hat{L}_\phi+\frac{N_B}{L_e}(1-2N_A)\hat{L}_\phi D+\frac{N_AN_B}{L_e}(D^2-a^2)D,$$

$$\hat{L}_T=\hat{D}^2-a^2-\gamma,\ \ \hat{\alpha}=PeG\left(\left(1+\alpha_0\right)D^2-\left(1-\alpha_0\right)a^2\right),$$

$$\hat{L}_D=D_a(D^2-a^2)-\gamma\mathcal{V}_a^{-1}-1,\ \hat{L}_\phi=D^2-a^2-\gamma\frac{L_e}{\tilde{\sigma}},$$

$$\hat{L}_N=\frac{1}{L_b}(D^2-a^2)-\frac{Pe}{L_b}D-\frac{\gamma}{\tilde{\sigma}},\ \hat{L}_B=\frac{Pr}{Pm}(D^2-a^2)-\frac{\gamma}{\tilde{\sigma}}.$$

Eq. (33) is supplemented with boundary conditions for free boundaries

$$W=D^2W=0\quad at\quad z=0,1. \tag{36}$$

Equation (35) describes bioconvection in a layer of a porous medium saturated by an electrically conducting nanofluid in an external vertical magnetic field. Further, we will use a single term approximation of Galerkin method to solve (35).

3. OSCILLATING AND STATIONARY CONVECTION REGIMES

The eigenfunctions W of equation (35) take the form of a simple harmonic for free boundary conditions (39):

$$W=W_0\sin\pi z, \tag{37}$$

where W_0 is constant. By substituting (40) for (38) and integrating across the layer thickness $z=(0,1)$, the characteristic equation is obtained, with Rayleigh number Ra as the eigenvalue:

$$\begin{gathered}Ra=\left(\frac{\left(\pi^2+a^2\right)\Gamma_D\Gamma_T}{a^2}+\frac{QPr}{\varepsilon Pm}\frac{\Gamma_T}{a^2\Gamma_B}\pi^2\left(\pi^2+a^2\right)\right)\frac{\left(1+P_{N_2}\right)}{\left(1-\dfrac{P_{N_1}}{\Gamma_\phi}\right)}-\\ -\frac{R_n}{\Gamma_\phi-P_{N_1}}\left(\frac{L_e}{\varepsilon}\Gamma_T+N_A\left(\pi^2+a^2\right)+P_{N_1}\left(1-2N_A\right)\right)-\frac{\left(\dfrac{R_b}{L_b}\right)\Gamma_\alpha\Gamma_T}{\Gamma_N\left(1-\dfrac{P_{N_1}}{\Gamma_\phi}\right)},\end{gathered} \tag{38}$$

where

$$\Gamma_D=D_a(\pi^2+a^2)+\gamma\mathcal{V}_a^{-1}+1,\ \Gamma_T=\pi^2+a^2+\gamma,\ \Gamma_N=\frac{1}{L_b}(\pi^2+a^2)+\frac{\gamma}{\tilde{\sigma}},$$

$$P_{N_1}=\frac{\pi^2N_BPe}{\varepsilon L_b\Gamma_N},\ P_{N_2}=1+\frac{\varepsilon P_{N_1}}{\Gamma_TL_e}\left(1-2N_A+\frac{N_A}{\Gamma_\phi}(\pi^2+a^2)\right),$$

$$\Gamma_B=\frac{Pr}{Pm}(\pi^2+a^2)+\frac{\gamma}{\tilde{\sigma}},\ \Gamma_\alpha=PeG\left(\left(1+\alpha_0\right)\pi^2+\left(1-\alpha_0\right)a^2\right).$$

For most nanofluids, the quantities $Pe\dfrac{N_B}{L_e},Pe\dfrac{N_B}{\varepsilon}$ are small ($N_B=7.5\cdot10^{-4}$, $L_e=5000$ see, for example, [5]), and expression (38) becomes simpler

$$Ra=\frac{(\pi^2+a^2)\Gamma_D\Gamma_T}{a^2}+\frac{QPr}{\varepsilon Pm}\frac{\Gamma_T}{a^2\Gamma_B}\pi^2(\pi^2+a^2)-\frac{R_n}{\Gamma_\phi}\left(\frac{L_e}{\varepsilon}\Gamma_T+N_A(\pi^2+a^2)\right)-\frac{\left(\frac{R_b}{L_b}\right)\Gamma_\alpha\Gamma_T}{\Gamma_N} \tag{39}$$

In the equation (39) the growth rate γ of perturbations is generally complex $\gamma=\gamma_r+i\omega_i$. It is obvious that the system is stable if $\gamma_r<0$ and unstable if $\gamma_r>0$. Let us determine the stability boundary for monotonic $\omega_i=0$ and oscillatory $\omega_i\neq 0$ perturbations. At the stability boundary (neutral states), $\gamma_r=0$; therefore, making the substitution $\gamma=i\omega_i$ in Eq. (39), we find

$$Ra=Ra^{(r)}+i\omega_i Ra^{(i)}, \tag{40}$$

where $Ra^{(r)}$ and $Ra^{(i)}$ are the real and imaginary parts of the dispersion equation for Ra:

$$\begin{aligned}Ra^{(r)}=&\frac{\left(\pi^2+a^2\right)}{a^2}\left(\left(D_a\left(\pi^2+a^2\right)+1\right)\left(\pi^2+a^2\right)-\omega_i^2\mathcal{V}_a^{-1}\right)+\frac{QPr}{\varepsilon Pm}\frac{\pi^2\left(\pi^2+a^2\right)}{a^2}\cdot\frac{\frac{Pr}{Pm}\left(\pi^2+a^2\right)^2+\frac{\omega_i^2}{\tilde\sigma}}{\frac{Pr^2}{Pm^2}\left(\pi^2+a^2\right)^2+\frac{\omega_i^2}{\tilde\sigma^2}}-\\&-\frac{R_n}{\left(\pi^2+a^2\right)^2+\frac{\omega_i^2L_e^2}{\tilde\sigma^2}}\left(\frac{L_e}{\varepsilon}\left(\left(\pi^2+a^2\right)^2+\frac{\omega_i^2L_e}{\tilde\sigma}\right)+N_A\left(\pi^2+a^2\right)^2\right)-\\&-Ra_B\left(\pi^2+a^2+\alpha_0\left(\pi^2-a^2\right)\right)\cdot\frac{\left(\pi^2+a^2\right)^2+\frac{\omega_i^2L_b}{\tilde\sigma^2}}{\left(\pi^2+a^2\right)^2+\frac{\omega_i^2L_b^2}{\tilde\sigma^2}}\end{aligned} \tag{41}$$

where $Ra_B=R_bPeG$ is the modified bioconvection Rayleigh-Darcy number.

$$\begin{aligned}Ra^{(i)}=&\frac{\left(\pi^2+a^2\right)}{a^2}\left(D_a\left(\pi^2+a^2\right)+1+\mathcal{V}_a^{-1}\left(\pi^2+a^2\right)\right)+\frac{QPr}{\varepsilon Pm}\frac{\pi^2\left(\pi^2+a^2\right)^2}{a^2}\cdot\frac{\frac{\tilde\sigma Pr-Pm}{\tilde\sigma Pm}}{\frac{Pr^2}{Pm^2}\left(\pi^2+a^2\right)^2+\frac{\omega_i^2}{\tilde\sigma^2}}-\\&-\frac{R_nL_e\left(\pi^2+a^2\right)}{\left(\pi^2+a^2\right)^2+\frac{\omega_i^2L_e^2}{\tilde\sigma^2}}\left(\frac{\tilde\sigma\left(\tilde\sigma-L_e\right)-\varepsilon N_A}{\varepsilon\tilde\sigma}\right)-\frac{Ra_B\left(\pi^2+a^2+\alpha_0\left(\pi^2-a^2\right)\right)}{\left(\pi^2+a^2\right)^2+\frac{\omega_i^2L_b^2}{\tilde\sigma^2}}\left(\frac{\tilde\sigma-L_b}{\tilde\sigma L_b}\right)\end{aligned} \tag{42}$$

Since the value Ra is real, then the imaginary part in (40) must vanish. In this case, the following situation $\omega_i=0$ or $Ra^{(i)}=0$ is possible.

4.1. Oscillating convection regime

In the case of an oscillatory perturbation $\omega_i\neq 0$ ($Ra^{(i)}=0$), we find the critical Rayleigh-Darcy number for oscillatory instability using the formula (41)

$$\begin{aligned}Ra_{osc}=&\frac{(\pi^2+a^2)}{a^2}\left(\left(D_a\left(\pi^2+a^2\right)+1\right)\left(\pi^2+a^2\right)-\omega_i^2\mathcal{V}_a^{-1}\right)+\frac{QPr}{\varepsilon Pm}\frac{\pi^2\left(\pi^2+a^2\right)}{a^2}\cdot\frac{\frac{Pr}{Pm}\left(\pi^2+a^2\right)^2+\frac{\omega_i^2}{\tilde\sigma}}{\frac{Pr^2}{Pm^2}\left(\pi^2+a^2\right)^2+\frac{\omega_i^2}{\tilde\sigma^2}}-\\&-\frac{R_n}{\left(\pi^2+a^2\right)^2+\frac{\omega_i^2L_e^2}{\tilde\sigma^2}}\left(\frac{L_e}{\varepsilon}\left(\left(\pi^2+a^2\right)^2+\frac{\omega_i^2L_e}{\tilde\sigma}\right)+N_A\left(\pi^2+a^2\right)^2\right)-Ra_B\left(\pi^2+a^2+\alpha_0\left(\pi^2-a^2\right)\right)\cdot\frac{\left(\pi^2+a^2\right)^2+\frac{\omega_i^2L_b}{\tilde\sigma^2}}{\left(\pi^2+a^2\right)^2+\frac{\omega_i^2L_b^2}{\tilde\sigma^2}}\end{aligned} \tag{43}$$

and the frequency of neutral oscillations $\omega = \omega_i$, satisfying the following equation:

$$\kappa_0\left(\frac{\omega}{\tilde{\sigma}}\right)^6 + \kappa_1\left(\frac{\omega}{\tilde{\sigma}}\right)^4 + \kappa_2\left(\frac{\omega}{\tilde{\sigma}}\right)^2 + \kappa_3 = 0, \tag{44}$$

where the following notation has been introduced:

$$\kappa_0 = q\cdot\, L_e^2 L_b^2,\ p = \frac{(\pi^2+a^2)}{a^2}\left((\pi^2+a^2)(D_a+\mathcal{V}_a^{-1})+1\right),$$

$$\kappa_1 = p(\pi^2+a^2)^2\left(L_e^2+L_b^2+\frac{Pr^2}{Pm^2}L_e^2L_b^2\right)+qL_e^2L_b^2-(r_nL_b^2+r_BL_e^2),\ q=\frac{QPr}{\varepsilon Pm}\frac{\pi^2(\pi^2+a^2)^2}{a^2}\frac{\tilde{\sigma}Pr-Pm}{\tilde{\sigma}Pm},$$

$$r_n = \frac{R_n(\pi^2+a^2)L_e}{\varepsilon\tilde{\sigma}}(\tilde{\sigma}(\tilde{\sigma}-L_e)-\varepsilon N_A),\ r_B=\frac{Ra_B(\tilde{\sigma}-L_b)}{\tilde{\sigma}L_b}(\pi^2+a^2+\alpha_0(\pi^2-a^2)),$$

$$\kappa_2 = p\left(\pi^2+a^2\right)^4\left(1+\frac{Pr^2}{Pm^2}(L_e^2+L_b^2)\right)+q\left(\pi^2+a^2\right)^2\left(L_e^2+L_b^2\right)-$$
$$-\left(\pi^2+a^2\right)^2\left(r_n\left(1+\frac{Pr^2}{Pm^2}L_b^2\right)+r_B\left(1+\frac{Pr^2}{Pm^2}L_e^2\right)\right)$$

$$\kappa_3 = p\left(\pi^2+a^2\right)^5\frac{Pr^2}{Pm^2}+q\left(\pi^2+a^2\right)^4-\frac{Pr^2}{Pm^2}\left(\pi^2+a^2\right)^4\left(r_n+r_B\right).$$

Equation (44) is cubic in ω^2, so it can lead to more than one positive value of ω^2 for fixed values of the parameters $D_a,\mathcal{V}_a,Q,Pr,Pm,\tilde{\sigma},R_n,L_e,N_A,L_b,Ra_B$ and α_0. If there are no positive solutions to Eq. (44), then oscillatory instability is impossible. Our numerical solution of Eq. (44) for the range of parameters considered here gives only a negative value of ω^2, which indicates the impossibility of an oscillatory neutral solution. As a result, we'll go through the stationary convection regime in significant detail.

4.2. Stationary convection regime

The marginal state will be characterized by $\omega_i = 0$, and the dispersion relation (41) reduces to

$$Ra_{st} = \frac{1}{a^2}\left(D_a(\pi^2+a^2)^3+(\pi^2+a^2)^2+\frac{\pi^2Q}{\varepsilon}(\pi^2+a^2)\right)-$$
$$-R_n\left(\frac{L_e}{\varepsilon}+N_A\right)-R_bPeG\left(\pi^2+a^2+\alpha_0\left(\pi^2-a^2\right)\right) \tag{45}$$

The last term in (45) describes a new effect of the influence of the motion of gyrotactic microorganisms on thermal instability. Thus, we have obtained a new way to control magnetic convection in a porous medium saturated with nanofluid using bioconvection of gyrotactic microorganisms.

Let us now continue to a more exhaustive analysis of the equation (45). The critical wave numbers for the onset of convection are found from the condition

$$\left(\frac{\partial Ra_{st}}{\partial a}\right)_{a=a_{cr}} = 0 \tag{46}$$

We get an equation for determining a_{cr} by substituting the expression (45) into the condition (46). This equation has a rather cumbersome form, so we do not present it here. However, we can conclude that the critical wave number a_{cr} does not depend on the nanofluid parameters (R_n,L_e,N_A), but depends on the dimensionless parameters $\varepsilon,D_a,Q,R_b,Pe,G,\alpha_0$. We will be doing a numerical study of the dispersion equation (45) using the physical characteristics of the Al_2O_3-water nanofluid from [5]:

$$\phi_0 = 0.001,\ \rho_f = 1000kg/m^3\ ,\ \mu = 10^{-3}Pas, \tag{47}$$

$$\rho_d = 4\cdot 10^3 kg/m^3,\ \alpha_m = 2\cdot 10^{-7} m^2/s,\ \beta = 3.4\cdot 10^{-3} 1/K,$$

$$D_B = 4\cdot 10^{-11} m^2/s,\ D_T = 6\cdot 10^{-11} m^2/s,$$

$$(\rho c)_p = 3.1\cdot 10^6 J/m^3,\ (\rho c)_f = 4\cdot 10^6 J/m^3,$$

$$T_d - T_u = 1K,\ T_u = 300K,\ L_e = 5000,\ \rho_p = 4\cdot 10^3 kg/m^3.$$

The above-mentioned parameter values give the following dimensionless parameter values: $L_e = 5000, Pr = 5$, and $N_A = 5$. The concentration Rayleigh-Darcy and bioconvection Rayleigh-Darcy numbers can be changed by varying the distance between the borders and the nanoparticle and microorganisms volumetric concentration. For a complete numerical analysis, we need the estimated parameters of gyrotactic microorganisms, for example, for the alga *Chlamydomonas nivalis* [20]:

$$D_m = 5\cdot 10^{-4} cm^2/s,\ N_0 = 10^6 cm^{-3},\ (\delta\rho)/\rho_0 = 5\cdot 10^{-2}, \tag{48}$$

$$\mathcal{V} = 5\cdot 10^{-10} cm^3,\quad W_c = 10^{-2} cm/s.$$

Next, we will fix the value for the parameter R_n as $R_n = 0.122$ and R_b as $R_b = 1.2\cdot 10^5$. The values of the parameters Pe and G change in the neighborhood of $Pe = 0.1$ and $G = 0.01$ [34]. The cell eccentricity can change in the range $\alpha_0 \in [0,1]$ [20].

In addition, we will be doing a numerical study of the dispersion equation (45) using the physical characteristics of nanofluids from metallic and semiconductor nanoparticles. Yang et al. [42] found that the physical characteristics of nanofluids change with the form, size, and volumetric percentage of nanoparticles. Metallic nanofluids, as the name implies, are metallic nanoparticles dispersed in a base fluid. Because metallic nanoparticles have a high thermal conductivity, they increase the thermal conductivity of nanofluids. We consider nanoparticles of metals (Cu and Ag) dispersed in the base fluid water for analyzing the stability of metallic nanofluids. For Cu-water nanofluid, the values of nanofluid parameters at $\delta\phi = \phi_u - \phi_d = 0.001$ (nanoparticle concentration) are $R_n = 0.392$, $N_A = 0.5$, $L_e = 5000$, and for Ag-water nanofluid: $R_n = 0.465$, $N_A = 0.5$, $L_e = 5000$ [16]. The electrical conductivity of semiconductor materials is approximately between a conductor and an insulator. At $\delta\phi = 0.001$ (nanoparticle concentration), the values of nanofluid parameters are $R_n = 0.159$, $N_A = 20$, $L_e = 5000$ for TiO_2-water nanofluid and $R_n = 0.0785$, $N_A = 17.5$, $L_e = 5000$ for SiO_2-water nanofluid [16].

5. WEAK NONLINEAR STABILITY ANALYSIS

We explored linear stability analysis using the normal mode method in the previous section. Although linear stability analysis is appropriate for studying the stability condition of the motionless solution describing convective flow. However, this approach cannot offer information regarding convection amplitudes and hence heat and mass transfer rates. In this section, we consider the situation of two-dimensional rolls, assuming that all physical variables are independent of y. In this case, Eqs. (1) and (7) for velocity and magnetic field perturbations will take the form

$$\frac{\partial u'}{\partial x} + \frac{\partial w'}{\partial z} = 0,\quad \frac{\partial b_x'}{\partial x} + \frac{\partial b_z'}{\partial z} = 0. \tag{49}$$

We may introduce two scalar functions using Eq. (49), the hydrodynamic function of the current ψ and the magnetic function Φ, for which the following relationships hold:

$$u' = \frac{\partial\psi}{\partial z},\quad w' = -\frac{\partial\psi}{\partial x},\quad b_x' = \frac{\partial\Phi}{\partial z},\quad b_z' = -\frac{\partial\Phi}{\partial x}. \tag{50}$$

Then equations (2)-(6) for the perturbed quantities, taking into account nonlinear effects, take the following form for dimensionless variables

$$\frac{1}{\varepsilon}\frac{\partial\psi}{\partial x} + \frac{1}{L_e}\nabla_1^2\phi' + \frac{N_A}{L_e}\nabla_1^2 T' = \frac{1}{\tilde{\sigma}}\frac{\partial\phi'}{\partial t} - \frac{1}{\varepsilon}\frac{\partial(\psi,\phi')}{\partial(x,z)}, \tag{51}$$

$$\frac{1}{L_b}\nabla_1^2 N' - \frac{Pe}{L_b}\frac{\partial N'}{\partial z} - PeG\frac{\partial \zeta}{\partial x} = \frac{1}{\tilde{\sigma}}\frac{\partial N'}{\partial t} - \frac{1}{\varepsilon}\frac{\partial(\psi, N')}{\partial(x,z)} + PeG\zeta\frac{\partial N'}{\partial x} + PeGN'\frac{\partial \zeta}{\partial x} \tag{52}$$

$$\nabla_1^2\psi - D_a\nabla_1^4\psi + Ra\frac{\partial T'}{\partial x} - R_n\frac{\partial \phi'}{\partial x} - \frac{R_b}{L_b}\frac{\partial N'}{\partial x} - \frac{QPr}{Pm}\frac{\partial}{\partial z}\nabla_1^2\Phi = -\frac{1}{\mathcal{V}_a}\frac{\partial}{\partial t}\nabla_1^2\psi - \frac{QPr}{Pm}\frac{\partial(\Phi, \nabla_1^2\Phi)}{\partial(x,z)} \tag{53}$$

$$\nabla_1^2 T' + \frac{N_B}{L_e}\left(\frac{\partial T'}{\partial z} - \frac{\partial \phi'}{\partial z}\right) - \frac{2N_A N_B}{L_e}\frac{\partial T'}{\partial z} - \frac{\partial \psi}{\partial x} = \frac{\partial T'}{\partial t} - \frac{\partial(\psi, T')}{\partial(x,z)} - \frac{N_B}{L_e}\left(\frac{\partial \phi'}{\partial x}\frac{\partial T'}{\partial x} + \frac{\partial \phi'}{\partial z}\frac{\partial T'}{\partial z}\right) -$$

$$-\frac{N_A N_B}{L_e}\left(\left(\frac{\partial T'}{\partial x}\right)^2 + \left(\frac{\partial T'}{\partial z}\right)^2\right), \tag{54}$$

$$\frac{1}{\varepsilon}\frac{\partial \psi}{\partial z} + \frac{Pr}{Pm}\nabla_1^2\Phi = \frac{1}{\tilde{\sigma}}\frac{\partial \Phi}{\partial t} - \frac{1}{\varepsilon}\frac{\partial(\psi, \Phi)}{\partial(x,z)}, \tag{55}$$

where

$$\nabla_1^2 = \frac{\partial^2}{\partial x^2} + \frac{\partial^2}{\partial z^2},\ \zeta = \nabla_1^2\psi + \alpha_0\left(\frac{\partial^2\psi}{\partial z^2} - \frac{\partial^2\psi}{\partial x^2}\right).$$

The boundary conditions considered for solving the given system of equations (51)-(55) are

$$\psi = D^2\psi = \Phi = D\Phi = \phi' = N' = T' = 0, \quad at \quad z = (0,1) \tag{56}$$

We use the following Fourier expressions to perform a local nonlinear stability analysis:

$$\begin{gathered}
\psi(x,z,t) = \sum_{n=1}^{\infty}\sum_{m=1}^{\infty} A_{mn}(t)\sin(mkx)\sin(n\pi z),\\
\Phi(x,z,t) = \sum_{n=1}^{\infty}\sum_{m=1}^{\infty} B_{mn}(t)\sin(mkx)\cos(n\pi z),\\
\phi'(x,z,t) = \sum_{n=1}^{\infty}\sum_{m=1}^{\infty} C_{mn}(t)\cos(mkx)\sin(n\pi z),\\
N'(x,z,t) = \sum_{n=1}^{\infty}\sum_{m=1}^{\infty} D_{mn}(t)\cos(mkx)\sin(n\pi z),\\
T'(x,z,t) = \sum_{n=1}^{\infty}\sum_{m=1}^{\infty} E_{mn}(t)\cos(mkx)\sin(n\pi z).
\end{gathered} \tag{57}$$

We limit our research with the Fourier analysis of the minimum order, namely, for the current function ψ and magnetic potential Φ we take the modes $(1,1)$, and $(1,1)+(0,2)$ for nanoparticle volume fraction, concentration of microorganisms (or cells), and temperature perturbations:

$$\begin{gathered}
\psi = A_{11}(t)\sin(kx)\sin(\pi z),\\
\Phi = B_{11}(t)\sin(kx)\cos(\pi z),\\
\phi' = C_{11}(t)\cos(kx)\sin(\pi z) + C_{02}(t)\sin(2\pi z),\\
N' = D_{11}(t)\cos(kx)\sin(\pi z) + D_{02}(t)\sin(2\pi z),\\
T' = E_{11}(t)\cos(kx)\sin(\pi z) + E_{02}(t)\sin(2\pi z).
\end{gathered} \tag{58}$$

The minimum order Fourier expansion was first used by Lorentz to model atmospheric convection [23]. The system of ordinary differential equations obtained by Lorentz is a low-order spectral model, but it is quite capable of qualitatively reproducing convective processes, in particular, the transition to a weakly turbulent state (chaos) through a series of bifurcations. In this study, we also use the Lorentz approach in describing the weakly nonlinear stage of convective instability. However, we do not touch upon issues related to the chaotic behavior of the obtained system of ordinary differential equations (51)-(55) since it requires a particular study. So we apply the weakly nonlinear theory

[43]-[45] to the problem of determining the characteristics of heat and mass transfer: nonstationary Nusselt $Nu(t)$ and Sherwood $Sh(t)$ numbers.

Substituting (58) in (51)-(55) and taking into account the orthogonality condition, we get the evolution equations for amplitudes:

$$\frac{\partial A_{11}}{\partial t} = -\mathcal{V}_a(1+D_a(k^2+\pi^2))A_{11} - \frac{kRa\mathcal{V}_a}{k^2+\pi^2}E_{11} + \frac{kR_n\mathcal{V}_a}{k^2+\pi^2}C_{11} + \frac{kR_b\mathcal{V}_a}{L_b(k^2+\pi^2)}D_{11} - \frac{\pi QPr\mathcal{V}_a}{Pm}B_{11}, \tag{59}$$

$$\frac{\partial B_{11}}{\partial t} = -\tilde{\sigma}(k^2+\pi^2)\frac{Pr}{Pm}B_{11} + \frac{\pi\tilde{\sigma}}{\varepsilon}A_{11}, \tag{60}$$

$$\frac{\partial C_{11}}{\partial t} = -\frac{\tilde{\sigma}}{L_e}(k^2+\pi^2)C_{11} - \frac{N_A}{L_e}\tilde{\sigma}(k^2+\pi^2)E_{11} + \frac{k\tilde{\sigma}}{\varepsilon}A_{11} - \frac{k\pi\tilde{\sigma}}{\varepsilon}A_{11}C_{02}, \tag{61}$$

$$\frac{\partial C_{02}}{\partial t} = -\frac{4\pi^2\tilde{\sigma}}{L_e}C_{02} - \frac{N_A}{L_e}4\pi^2\tilde{\sigma}E_{02} + \frac{k\pi\tilde{\sigma}}{2\varepsilon}A_{11}C_{11}, \tag{62}$$

$$\frac{\partial D_{11}}{\partial t} = -\frac{\tilde{\sigma}}{L_b}\left(k^2+\pi^2\right)D_{11} - \frac{k\pi\tilde{\sigma}}{\varepsilon}A_{11}D_{02} + PeG\tilde{\sigma}k\left(k^2+\pi^2+\alpha_0\left(\pi^2-k^2\right)\right)A_{11}, \tag{63}$$

$$\frac{\partial D_{02}}{\partial t} = -\frac{4\pi^2\tilde{\sigma}}{L_b}D_{02} + \frac{k\pi\tilde{\sigma}}{2\varepsilon}A_{11}D_{11}, \tag{64}$$

$$\frac{\partial E_{11}}{\partial t} = -(k^2+\pi^2)E_{11} - kA_{11} - \pi kA_{11}E_{02}, \tag{65}$$

$$\frac{\partial E_{02}}{\partial t} = -4\pi^2E_{02} + \frac{k\pi}{2}A_{11}E_{11}. \tag{66}$$

In phase space, the eight-mode differential Eqs. (59)-(66) have an interesting property that indicates that the system is dissipative:

$$\begin{aligned}&\frac{\partial\dot{A}_{11}}{\partial A_{11}} + \frac{\partial\dot{B}_{11}}{\partial B_{11}} + \frac{\partial\dot{C}_{11}}{\partial C_{11}} + \frac{\partial\dot{C}_{02}}{\partial C_{02}} + \frac{\partial\dot{D}_{11}}{\partial D_{11}} + \frac{\partial\dot{D}_{02}}{\partial D_{02}} + \frac{\partial\dot{E}_{11}}{\partial E_{11}} + \frac{\partial\dot{E}_{02}}{\partial E_{02}} = \\ &= -\mathcal{V}_a\left(1+D_a\left(k^2+\pi^2\right)\right) - \tilde{\sigma}\left(k^2+\pi^2\right)\left(\frac{Pr}{Pm}+\frac{1}{L_e}+\frac{1}{L_b}\right) - 4\pi^2\tilde{\sigma}\left(\frac{1}{L_e}+\frac{1}{L_b}\right) - \left(k^2+\pi^2\right) - 4\pi^2 < 0\end{aligned} \tag{67}$$

As a result, the impact of parameters $R_n, R_b, L_e, N_A, L_b, \mathcal{V}_a$ on trajectories is to attract them to a set of measures zero, or a fixed point. For the time-dependent variables, the nonlinear system of differential equations cannot be solved analytically and must be solved numerically. In the case of steady motions, Eqs. (59)-(66) become:

$$\begin{aligned}&A_{11} = \frac{1}{1+D_a\left(k^2+\pi^2\right)}\left[-\frac{kRa}{k^2+\pi^2}E_{11} + \frac{kR_n}{k^2+\pi^2}C_{11} + \frac{kR_b}{L_b\left(k^2+\pi^2\right)}D_{11} - \frac{\pi QPr}{Pm}B_{11}\right],\\ &B_{11} = \frac{\pi Pm}{Pr\left(k^2+\pi^2\right)}A_{11},\quad C_{11} = -N_AE_{11} + \frac{kL_e}{\varepsilon\left(k^2+\pi^2\right)}A_{11} - \frac{k\pi L_e}{\varepsilon\left(k^2+\pi^2\right)}A_{11}C_{02},\\ &C_{02} = -N_AE_{02} + \frac{kL_e}{8\pi\varepsilon}A_{11}C_{11},\quad D_{11} = -\frac{k\pi L_b}{\varepsilon\left(k^2+\pi^2\right)}A_{11}D_{02} + \frac{kPeGL_b}{k^2+\pi^2}\left(k^2+\pi^2+\alpha_0\left(\pi^2-k^2\right)\right)A_{11},\\ &D_{02} = \frac{kL_b}{8\pi\varepsilon}A_{11}D_{11},\quad E_{11} = -\frac{k}{k^2+\pi^2}A_{11} - \frac{k\pi}{k^2+\pi^2}A_{11}E_{02},\quad E_{02} = \frac{k}{8\pi}A_{11}E_{11}.\end{aligned} \tag{68}$$

The steady state solutions are useful because they indicate that the system can have a finite amplitude solution. When all amplitudes except A_{11} are eliminated, an equation with $A_{11}^2/8$ is obtained:

$$\left(\frac{A_{11}^2}{8}\right)^3 + \beta_1\left(\frac{A_{11}^2}{8}\right)^2 + \beta_2\left(\frac{A_{11}^2}{8}\right) + \beta_3 = 0, \tag{69}$$

where

$$\beta_1=\frac{L_e^2+L_b^2}{k_1^2L_e^2L_b^2}+\frac{1}{k_0^2}-\frac{Ra}{k_0^2M}-\frac{R_n\left(\frac{1}{\varepsilon}-N_A\right)}{k_1^2L_eM}-\frac{Ra_B\left(k^2+\pi^2+\alpha_0\left(\pi^2-k^2\right)\right)}{k_1^2L_b^2M},$$

$$M=\frac{\left(1+D_a\left(k^2+\pi^2\right)\right)\left(k^2+\pi^2\right)^2}{k^2}+\frac{\pi^2Q\left(k^2+\pi^2\right)}{\varepsilon k^2},\ k_0=\frac{k^2}{k^2+\pi^2},\ k_1^2=\frac{k^2}{\varepsilon^2\left(k^2+\pi^2\right)},$$

$$\beta_2=\frac{k_0^2+k_1^2\left(L_e^2+L_b^2\right)}{k_0^2k_1^4L_e^2L_b^2}-\frac{Ra\left(L_e^2+L_b^2\right)}{k_0^2k_1^2L_e^2L_b^2M}-\frac{R_n\left(\frac{L_e}{\varepsilon}+N_A\right)}{k_0^2k_1^2L_e^2M}-$$

$$\frac{R_n\left(\frac{1}{\varepsilon}-N_A\right)}{k_1^4L_e^2L_b^2M}-\frac{Ra_B\left(k^2+\pi^2+\alpha_0\left(\pi^2-k^2\right)\right)}{k_0^2k_1^4L_e^2L_b^2M}\left(k_0^2+k_1^2L_e^2\right),\ \beta_3=\frac{Ra_{st}-Ra}{k_0^2k_1^4L_e^2L_b^2M}.$$

In the limit of small amplitudes $(A_{11}\to 0)$, Eq. (69) transforms into dispersion equation (45) for the stationary convection regime when the wave number a is replaced by k. It should be noted that the amplitude of the stream function must be real, hence we must only consider positive signs in the roots of Eq. (69). If we determine the value of A_{11}, we can find the value of heat and mass transfer in a stationary regime.

6. RESULTS AND DISCUSSIONS

6.1. Analysis of the linear regime of stationary convection

Now, we will study the effects of axial magnetic field, Darcy number, medium porosity, Lewis number, modified diffusivity ratio, concentration Rayleigh-Darcy number, modified bioconvection Rayleigh-Darcy number $Ra_B=R_bPeG$, and the cell eccentricity on thermal instability. We calculate the derivatives

$$\frac{dRa_{st}}{dQ},\frac{dRa_{st}}{dD_a},\frac{dRa_{st}}{d\varepsilon},\frac{dRa_{st}}{dL_e},\frac{dRa_{st}}{dN_A},\frac{dRa_{st}}{dR_n},\frac{dRa_{st}}{dRa_B},\frac{dRa_{st}}{d\alpha_0},$$

using Eq. (45), as a result we obtain

$$\frac{dRa_{st}}{dQ}=\frac{\pi^2(\pi^2+a^2)}{\varepsilon a^2}, \tag{70}$$

$$\frac{dRa_{st}}{dD_a}=\frac{(\pi^2+a^2)^3}{a^2}, \tag{71}$$

$$\frac{dRa_{st}}{d\varepsilon}=\frac{R_nN_AL_e}{\varepsilon^2}-\frac{\pi^2(\pi^2+a^2)Q}{\varepsilon^2a^2}, \tag{72}$$

$$\frac{dRa_{st}}{dL_e}=-\frac{R_n}{\varepsilon},\quad \frac{dRa_{st}}{dN_A}=-R_n,\quad \frac{dRa_{st}}{dR_n}=-\left(\frac{L_e}{\varepsilon}+N_A\right). \tag{73}$$

Eq. (70) shows that the derivative dRa_{st}/dQ is always positive, i.e. the vertical magnetic field has a stabilizing effect on stationary convection in the porous medium. As a consequence, it is discovered that increasing the magnetic field delays the initiation of convection, which is agreement with the results derived by Ahuja et al. [13].

Eq. (71) implies that the Darcy number has a stabilizing influence on the stationary convection of the system, which is in a good agreement with the results derived by Kuznetsov and Nield [7], Rana and Chand [11], Ahuja et al. [13]. With an increase in Darcy number, Ra_{st} increases, indicating that the heat transmission characteristics of the nanofluid will improve. Therefore, the effect of the Darcy number, as well as the magnetic field, delays the onset of convection.

Eq. (72) shows that porosity can have both a stabilizing and destabilizing effect. If inequality

$$\frac{R_nN_AL_e}{\varepsilon^2}>\frac{\pi^2\left(\pi^2+a^2\right)Q}{\varepsilon^2a^2}$$

is satisfied, then porosity delays the onset of convection. This conclusion is in good accord with Ahuja et al. [13] results.

The following conclusions may be drawn from Eq. (73). Because all of the parameters L_e, N_A, and R_n are positive for the current configuration of nanoparticles, and the expression $R_n(L_e/\varepsilon + N_A)$ appears with a negative sign, it is obvious that the suspension of nanoparticles in ordinary fluids decreases the critical value of Rayleigh number. As a result, the system with nanoparticle distribution at the top of the fluid layer is less stable than the system with regular fluid and bottom heavy nanoparticle distribution.

Finally, we proceed to study the impact of gyrotactic microorganism bioconvection on magnetic convection. For this purpose, we calculate the following derivatives

$$\frac{dRa_{st}}{dRa_B} = -\left[\pi^2 + a^2 + \alpha_0\left(\pi^2 - a^2\right)\right], \tag{74}$$

$$\frac{dRa_{st}}{d\alpha_0} = -Ra_B(\pi^2 - a^2). \tag{75}$$

Eq. (74) shows that the spherical shape of microorganisms $\alpha_0 = 0$ contributes has a destabilizing effect since

$$\frac{dRa_{st}}{dRa_B} = -(\pi^2 + a^2) < 0 \tag{76}$$

Thus, increasing the value of modified bioconvection Rayleigh-Darcy number Ra_B enhances the magnetic convection nanofluid in the layer of a porous medium. In the case of an arbitrary form of microorganisms, an increase in the parameter Ra_B can both stabilize (at $\pi^2 + a^2 < \alpha_0(a^2 - \pi^2)$) and destabilize (at $\pi^2 + a^2 > \alpha_0(a^2 - \pi^2)$) the thermal instability if α_0 is positive: $\alpha_0 > 0$.

Eq. (75) shows that $dRa_{st}/d\alpha_0$ can be positive or negative, i.e. the cell (or microorganism) eccentricity has a stabilizing (if $\pi^2 < a^2$) or destabilizing (if $\pi^2 > a^2$) effect on stationary convection. This conclusion remains valid for positive $Ra_B > 0$ numbers.

6.2. Heat and mass transports

The determination of heat and mass transport is critical in the study of fluid convection. This is because the onset of convection, when the Rayleigh number increases, is more easily observed through its influence on heat and mass transport. Consequently, heat and mass fluxes of nanoparticles are important in identifying thermal- and bioconvective motion in its early stages. Heat transfers can be calculated and described using the Nusselt number $Nu(t)$ (see, for example [45])

$$Nu(t) = 1 + \left[\frac{\int_0^{2\pi/k_{cr}} \frac{\partial T'}{\partial z} dx}{\int_0^{2\pi/k_{cr}} \frac{\partial T_b}{\partial z} dx}\right]_{z=0} \tag{77}$$

According to (22) and (57), we get from (77)

$$Nu(t) = 1 - 2\pi E_{02}(t) \tag{78}$$

Similarly, the Sherwood number for nanoparticle concentration $Sh(t)$ is determined to be:

$$Sh(t) = 1 + \left[\frac{\int_0^{2\pi/k_{cr}} \frac{\partial \phi'}{\partial z} dx}{\int_0^{2\pi/k_{cr}} \frac{\partial \phi_b}{\partial z} dx}\right]_{z=0} = 1 + 2\pi C_{02}(t) \tag{79}$$

In the next section, we will consider the numerical/graphical investigation of the equations (70)-(79) by considering the numerical values of various parameters of the system.

7. NUMERICAL RESULTS AND DISCUSSION

In this section, we use the standard Maple computer environment programs for the numerical analysis of equations (70)-(75) and (78)-(79). Nonlinear equations (59)-(66) were solved by the 4th-5th order Runge-Kutta-Felberg method (rfk45) with initial conditions:

$$A_{11}(0) = B_{11}(0) = C_{11}(0) = C_{02}(0) = D_{11}(0) = D_{02}(0) = E_{11}(0) = E_{02}(0) = 1.$$

7.1. Stationary MHD bioconvection in Al_2O_3-water nanofluid

Figures 2 and 3 depict the role of the magnetic field, Darcy parameter, porosity, Lewis number, modified diffusivity ratio, nanoparticles concentration Rayleigh number, modified bioconvection Rayleigh-Darcy number, and cell (or microorganism) eccentricity α_0 on Rayleigh number for metal oxide (Al_2O_3) nanoparticles in water based nanofluid. The physical properties of aluminum-water nanofluids are given in (47).

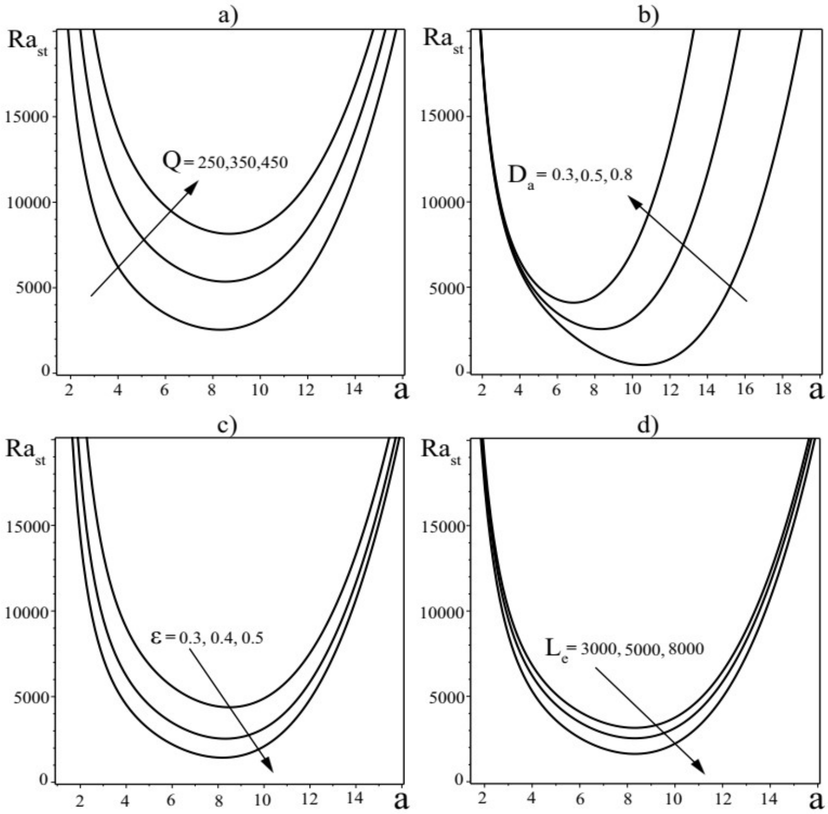

Figure 2. Dependence of the Rayleigh number of stationary convection on the wavenumber a for parameter variations: (a) magnetic field (Chandrasekhar number) Q; (b) Darcy number D_a; (c) medium porosity ε; (d) Lewis number L_e

In Fig. 2a, the Rayleigh-Darcy number is plotted against the dimensionless wavenumber for different values of the axial magnetic field (Chandrasekhar number). This shows that as values of axial magnetic field increase, the Rayleigh-Darcy number also increases for fixed values

$$D_a = 0.5, \varepsilon = 0.4, L_e = 5000, N_A = 5, R_n = 0.122, Ra_B = 120, \alpha_0 = 0.4 .$$

As a consequence, the axial magnetic field can stabilize stationary convection, which is consistent with the analytical conclusion obtained from Eq. (70).

For different values of the Darcy number, the Rayleigh-Darcy number is displayed against the dimensionless wavenumber in Fig. 2b for fixed values

$$Q = 250, \varepsilon = 0.4, L_e = 5000, N_A = 5, R_n = 0.122, Ra_B = 120, \alpha_0 = 0.4 .$$

This demonstrates that when Darcy's number rises, so does the Rayleigh-Darcy number. As a result, the Darcy number has a stabilizing impact on stationary convection, which is in agreement with the analytical result obtained from Eq. (71).

For different values of medium porosity, the Rayleigh-Darcy number is plotted against dimensionless wavenumber in Fig. 2c for fixed values

$$D_a = 0.5, Q = 250, L_e = 5000, N_A = 5, R_n = 0.122, Ra_B = 120, \alpha_0 = 0.4 .$$

This shows that when porosity increases, the values of Rac decrease significantly. As a result, medium porosity has a destabilizing impact on stationary convection, which is consistent with the analytical result obtained from Eq. (72).

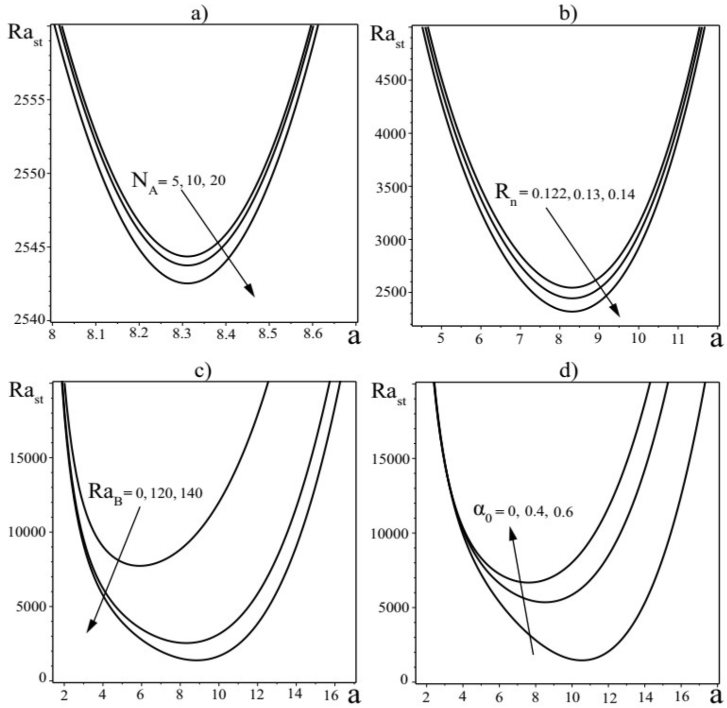

Figure 3. Dependence of the Rayleigh number of stationary convection on the wavenumber a for parameter variations: (a) modified diffusivity ratio N_A ; (b) concentration Rayleigh-Darcy number R_n ; (c) modified bioconvection Rayleigh-Darcy number Ra_B ; (d) cell eccentricity α_0

In Figs. 2d, 3a, 3b the Rayleigh-Darcy number is plotted against dimensionless wavenumber for different values of Lewis number, modified diffusivity ratio, and concentration Rayleigh number. These show that as Lewis number, modified diffusivity ratio, and concentration Rayleigh number increase, the Rayleigh-Darcy numbers decrease. Thus, the nanofluid parameters have a destabilizing effect on stationary convection, which is in good agreement with the result obtained analytically from Eqs. (73).

In Fig. 3c, the stationary Rayleigh-Darcy number Ra_{st} is plotted against dimensionless wave number a for different values of modified bioconvection Rayleigh-Darcy number Ra_B for fixed values $D_a = 0.5, Q = 250, \varepsilon = 0.4, L_e = 5000, N_A = 5, R_n = 0.122, \alpha_0 = 0.4$. Curve 1 depicts the dependency of the stationary Rayleigh-Darcy number on the wave number in the absence of the impact of microorganism bioconvection, i.e. when $R_b = 0$. A similar dependence also arises in the case when there is no gyrotax $G = 0$ ($Ra_B = 0$). The gyrotaxis number G characterizes the deviation of the cell's swimming direction from strictly vertical. If $G = 0$, there is no gyrotaxis and the microorganisms swim vertically upwards (show negative geotaxis). Pedley et al. [19] demonstrated that a suspension of gyrotactic microorganisms ($G > 0$) is unstable under the same conditions. As a result, gyrotaxis plays a role in the emergence of bioconvection instability. As can be seen from Fig. 3c, with an increase in the parameter Ra_B , the threshold for the occurrence of magnetic convection decreases. This is because the movement of microorganisms leads to a redistribution of the density of the nanofluid, reducing the process of heat transfer in the nanofluid. As a consequence, the cell's swimming can destabilize stationary magnetoconvection, which is consistent with the analytical conclusion obtained from Eq. (74).

Table 1. Critical Rayleigh numbers Ra_{st}^{min} and critical wavenumbers k_{cr} for Al_2O_3 -water nanofluid at fixed parameters $R_n = 0.122$, $N_A = 5$, $L_e = 5000$

Q	D_a	ε	Ra_B	α_0	Ra_{st}^{min}	k_{cr}
250	0.5	0.4	120	0.4	2544.36	8.31
350	0.5	0.4	120	0.4	5355.59	8.51
450	0.5	0.4	120	0.4	8151.92	8.69
250	0.3	0.4	120	0.4	445.25	10.57
250	0.5	0.4	120	0.4	2544.36	8.31
250	0.8	0.4	120	0.4	4095.58	6.86
250	0.5	0.3	120	0.4	4379.85	8.48
250	0.5	0.4	120	0.4	2544.36	8.31

Q	D_a	ε	Ra_B	α_0	Ra_{st}^{min}	k_{cr}
250	0.5	0.5	120	0.4	1436.89	8.19
250	0.5	0.4	0	No	7730.31	5.90
250	0.5	0.4	120	0.4	2544.36	8.31
250	0.5	0.4	140	0.4	1384.94	8.85
350	0.5	0.4	120	0	1459.64	5.32
350	0.5	0.4	120	0.4	5355.59	8.51
350	0.5	0.4	120	0.6	6675.31	7.60

In Fig. 3d, the stationary Rayleigh-Darcy number Ra_{st} is plotted against dimensionless wave number a for different values of cell eccentricity α_0 for fixed values $D_a = 0.5, Q = 350, \varepsilon = 0.4, L_e = 5000, N_A = 5, R_n = 0.122, Ra_B = 120$. As can be seen from Fig. 3d, the spherical shape of microorganisms has a destabilizing effect on the beginning of magnetoconvection. This conclusion is confirmed by analytical results Eqs. (75) and (76).

The critical Rayleigh numbers Ra_{st}^{min} and the corresponding critical wavenumbers a_{cr} for different values of $Q, D_a, \varepsilon, Ra_B$ and α_0 for Al_2O_3-water nanofluid are shown in Table 1. Let's notice that results in Table 1 were obtained numerically using (46) for Al_2O_3-water nanofluid and are in good agreement with the graphical results in Figs. 2a, 2b, 2c and Figs. 3c, 3d. In the limiting case when there are no microorganisms ($Ra_B = 0$), the results from Table 1 are in good agreement with the results of paper [18].

7.2. Stationary MHD bioconvection in Cu (Ag)-water and TiO_2 (SiO_2)-water nanofluids

We now consider the graphical interpretation of numerical calculations for metallic nanofluids (Cu, Ag) and semiconductors (TiO_2 and SiO_2). We investigate the impact of several nanofluids (metal, metal oxide, and semiconductor) on stationary convection by fixing the values of the parameters $Da, V_a, Q, Pr, Pm, \tilde{\sigma}, Le, Lb, Ra_B$ and α_0. The thermal Rayleigh-Darcy number Ra_{st} is plotted against the wavenumber for several nanofluids in Fig. 4. From Fig. 4, we can see that the SiO_2-water nanofluid exhibits the highest stability compared to Al_2O_3-water, TiO_2-water, Cu-water and Ag-water nanofluids. The phenomena for this behavior is not only the different density of nanoparticles but also different thermophysical properties. We can conclude that semiconductor and metal oxide nanoparticles have a more destabilizing effect on stationary convection than metallic nanoparticles.

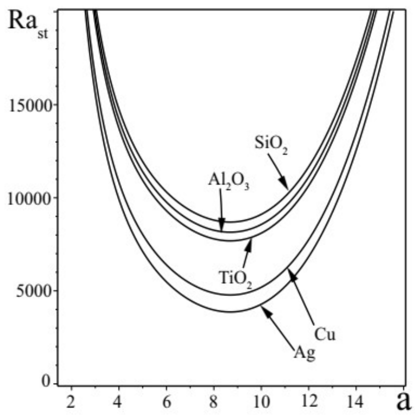

Figure 4. Dependence of the Rayleigh number of stationary convection on the wavenumber a for metal oxide (Al_2O_3), metallic (Cu, Ag), and semiconducting (TiO_2, SiO_2) nanoparticles in water based nanofluids ($D_a = 0.5, Q = 450, \varepsilon = 0.4, L_e = 5000, Ra_B = 120, \alpha_0 = 0.4$)

Let us now consider the impact of different nanofluid parameters on the thermal instability of the system under the simultaneous influence of magnetic field. Figures 5a and 5b illustrate the impact of the Chandrasekhar number on the Rayleigh-Darcy number for metals (Cu, Ag) and semiconductors (TiO_2, SiO_2) in water-based nanofluids. These figures show that when the value of the Chandrasekhar parameter Q increases, the values of the thermal Rayleigh-Darcy number for both forms of convection increase, indicating that magnetic field has a stabilizing impact. The curves depicting the influence of Chandrasekhar number for Cu-water nanofluid are above those for Ag-water nanofluid, indicating that Cu-water nanofluid is more stable than Ag-water nanofluid. When the situation of semiconductors is considered

(Fig. 5b), it is found that SiO_2-nanoparticles improve the stability of nanofluid more than TiO_2-nanoparticles as the Chandrasekhar number increases. Thus, it is also interpreted from the figures that semiconductors inhibit the onset of convection as compared to metals under the influence of magnetic field.

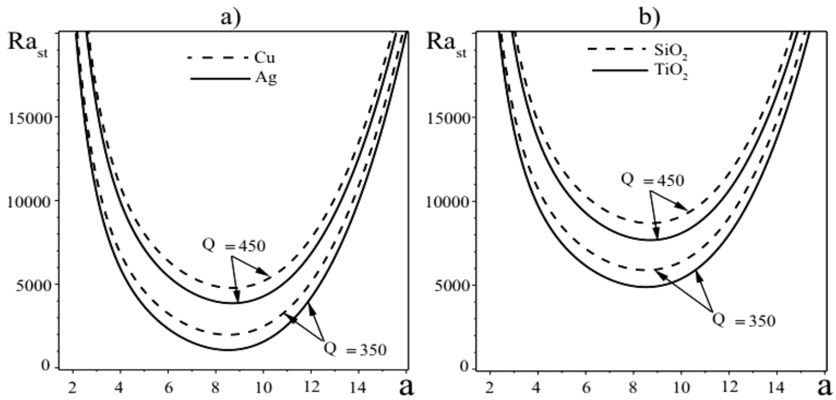

Figure 5. Impact of Chandrasekhar number Q on the stationary convective instability for different nanofluids: (a) Cu (Ag) - water; (b) TiO_2 (SiO_2)-water ($D_a = 0.5, \varepsilon = 0.4, L_e = 5000, Ra_B = 120, \alpha_0 = 0.4$)

Figures 6a and 6b show the effect of Darcy number on the system. The value of Ra_{st} increases with the increase in Darcy's number and hence the Darcy number D_a delays the onset of instability. By increasing the Darcy number Cu-water and SiO_2-water nanofluids exhibit higher stability than Ag-water and TiO_2-water nanofluids.

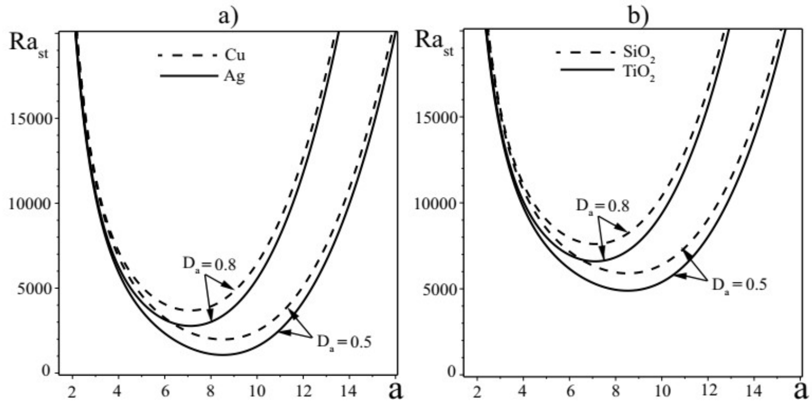

Figure 6. Impact of Darcy number D_a on the stationary convective instability for different nanofluids:
(a) Cu (Ag)-water; (b) TiO_2 (SiO_2)-water ($Q = 350, \varepsilon = 0.4, L_e = 5000, Ra_B = 120, \alpha_0 = 0.4$)

Further, let us study the influence of the effect of porosity on the system. Figures 7a and 7b show that the increase in ε porosity stimulates the onset of instability. The critical Rayleigh-Darcy numbers for nonmetallic nanofluids are higher than that for metallic nanofluids.

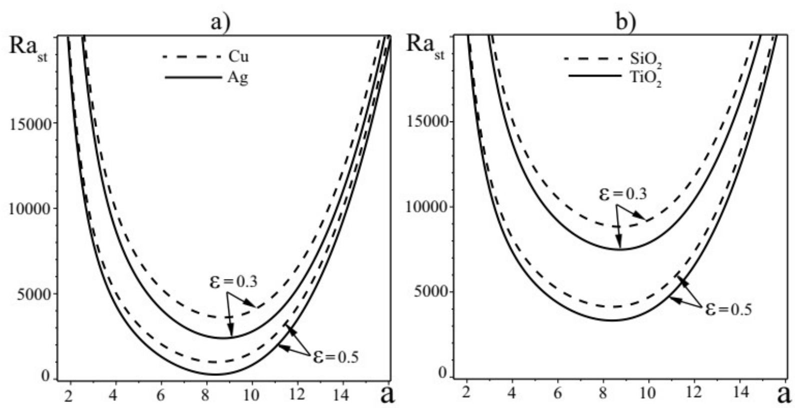

Figure 7. Impact of porosity ε on the stationary convective instability for different nanofluids:
(a) Cu (Ag)-water; (b) TiO_2 (SiO_2)-water ($D_a = 0.5, Q = 350, L_e = 5000, Ra_B = 120, \alpha_0 = 0.4$)

Figures 8a and 8b illustrate the impact of modified bioconvection Rayleigh-Darcy number Ra_B on the stationary convective instability for metallic and semiconductors nanofluids. We can observe that the cell's swimming can destabilize stationary magnetoconvection since the threshold for the occurrence of magnetic convection decreases when the parameter Ra_B is increased. As can be seen from Fig. 8 nonmetallic nanoparticles delay the onset of convection even in the absence of bioconvection $Ra_B = 0$ (or movement of microorganisms).

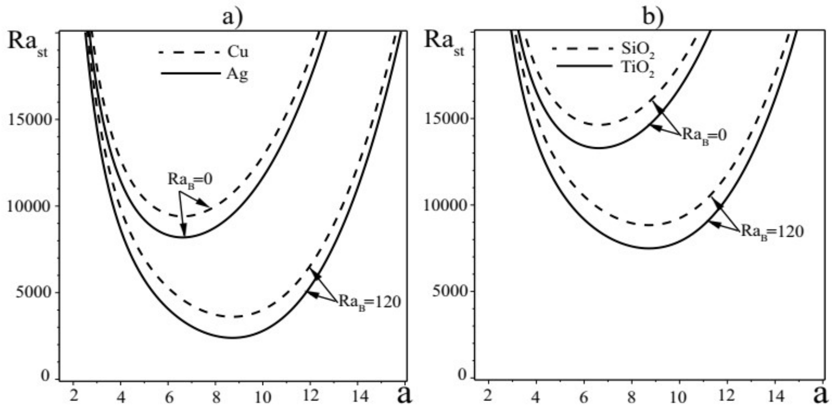

Figure 8. Impact of modified bioconvection Rayleigh-Darcy number Ra_B on the stationary convective instability for different nanofluids: (a) Cu (Ag)-water; (b) TiO_2 (SiO_2)-water ($D_a = 0.5, Q = 350, \varepsilon = 0.3, L_e = 5000, \alpha_0 = 0.4$)

Finally, let us study the influence of the effect of cell eccentricity α_0 on thermal stability. Figures 9a and 9b show that the spherical shape of microorganisms has a destabilizing effect on the beginning of magnetoconvection for metallic as for nonmetallic nanoparticles. However, nonmetallic nanoparticles still retard the development of stationary convection.

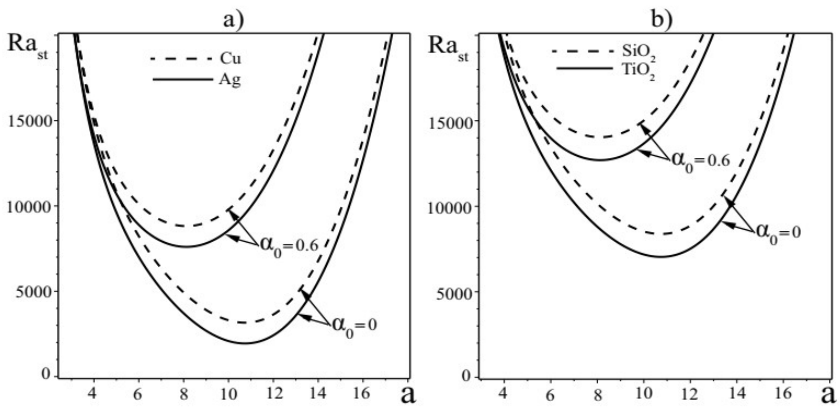

Figure 9. Impact of cell eccentricity α_0 on the stationary convective instability for different nanofluids: (a) Cu (Ag)-water; (b) TiO_2 (SiO_2)-water ($D_a = 0.5, Q = 450, \varepsilon = 0.3, L_e = 5000, Ra_B = 120$).

The critical Rayleigh numbers Ra_{st}^{min} and the corresponding critical wavenumbers a_{cr} for different values of $Q, D_a, \varepsilon, Ra_B$ and α_0 for metallic nanofluids (Cu -water, Ag -water) are shown in Table 2. Take note that the results in Table 2 were derived numerically using (46) for metallic nanofluids (Cu -water, Ag -water) and correspond well with the graphical results in Figs. 5a, 6a, 7a, 8a, 9a.

Table 2. The critical Rayleigh numbers Ra_{st}^{min} and critical wavenumbers k_{cr} for metallic nanofluids (Cu -water, Ag -water) at fixed parameters $L_e = 5000$, a) $R_n|_{Cu} = 0.392, N_A|_{Cu} = 0.5$, b) $R_n|_{Ag} = 0.465, N_A|_{Ag} = 0.5$

Q	D_a	ε	Ra_B	α_0	a) Ra_{st}^{min}	a) k_{cr}	b) Ra_{st}^{min}	b) k_{cr}
350	0.5	0.4	120	0.4	1981.01	8.51	1068.47	8.51
450	0.5	0.4	120	0.4	4777.34	8.69	3864.80	8.69
350	0.5	0.4	120	0.4	1981.01	8.51	1068.47	8.51
350	0.8	0.4	120	0.4	3686.96	7.11	2774.42	7.11
350	0.5	0.3	120	0.4	3608.82	8.71	2392.12	8.71

Q	D_a	ε	Ra_B	α_0	a) Ra_{st}^{min}	a) k_{cr}	b) Ra_{st}^{min}	b) k_{cr}
350	0.5	0.5	120	0.4	994.92	8.37	264.88	8.37
350	0.5	0.3	0	No	9406.12	6.61	8189.42	6.61
350	0.5	0.3	120	0.4	3608.82	8.71	2392.12	8.71
450	0.5	0.3	120	0	3157.93	10.73	1941.22	10.73
450	0.5	0.3	120	0.6	8817.45	8.12	7600.75	8.12

The critical Rayleigh numbers Ra_{st}^{min} and the corresponding critical wavenumbers a_{cr} for different values of $Q, D_a, \varepsilon, Ra_B$ and α_0 for semiconductor nanofluids (TiO_2 -water, SiO_2 -water) are shown in Table 3. We notice that the numerical results in Table 3 for semiconductor nanofluids (TiO_2 -water, SiO_2 -water) agree well to the graphical results in Figs. 5b, 6b, 7b, 8b, 9b. In the limited case of no microorganisms $(Ra_B = 0)$, the results from Tables 2 and 3 agree well with the results of paper [13].

Table 3. The critical Rayleigh numbers Ra_{st}^{min} and critical wavenumbers k_{cr} for semiconductor nanofluids (TiO_2 -water, SiO_2 -water) at fixed parameters $L_e = 5000$, a) $R_n|_{TiO_2} = 0.159, N_A|_{TiO_2} = 20$, b) $R_n|_{SiO_2} = 0.0785, N_A|_{SiO_2} = 17.5$

Q	D_a	ε	Ra_B	α_0	a) Ra_{st}^{min}	a) k_{cr}	b) Ra_{st}^{min}	b) k_{cr}
350	0.5	0.4	120	0.4	4890.52	8.51	5898.58	8.51
450	0.5	0.4	120	0.4	7686.86	8.69	8694.91	8.69
350	0.5	0.4	120	0.4	4890.52	8.51	5898.58	8.51
350	0.8	0.4	120	0.4	6596.47	7.11	7604.53	7.11
350	0.5	0.3	120	0.4	7489.17	8.71	8832.65	8.71
350	0.5	0.5	120	0.4	3321.94	8.37	4128.75	8.37
350	0.5	0.3	0	No	13286.47	6.61	14629.94	6.61
350	0.5	0.3	120	0.4	7489.17	8.71	8832.64	8.71
450	0.5	0.3	120	0	7038.28	10.73	8381.75	10.73
450	0.5	0.3	120	0.6	12697.80	8.12	14041.28	8.12

It is noteworthy that copper-water nanofluid is more stable than silver-water nanofluid (refer to Figures 5a, 6a, 7a, 8a, 9a) and silicon oxide-water nanofluid is more stable than titanium oxide-water nanofluid (refer to Figures 5b, 6b, 7b, 8b, 9b). These conclusions are consistent with the results of paper [14].

7.3. The numerical/graphical results for Nusselt $Nu(t)$ and Sherwood $Sh(t)$ numbers

In general, the transition from linear to non-linear convection can be complex. The study of Eqs. (59)-(66), whose solution provides a full description of the two dimensional non-linear evolution issues, helps to understand the transition. The Runge-Kutta technique is used to solve the autonomous system of unstable finite-amplitude equations. Convective heat and mass transfers were calculated using Nusselt number $Nu(t)$ and Sherwood number $Sh(t)$. The results are presented in Figures 10-12. It is assumed that the original value of the Nusselt and Sherwood number are equal to 1 at $t = 0$. These figures show that when time is short, oscillations in the values of the Nusselt and Sherwood numbers occur, indicating an unsteady rate of heat and mass transfer in the thermal convection system. These values approach a steady state, equivalent to a near convection stage, as time passes.

Figs. 10a-10h depict the temporary behavior of thermal Nusselt number $Nu(t)$, for varying values of magnetic field (Chandrasekhar number Q), Darcy number D_a, nanoparticle concentration Rayleigh-Darcy number R_n, bioconvection Rayleigh-Darcy number R_b, modified gyrotaxis number PeG, geometric shape of microorganisms α_0 and bioconvection Lewis number L_b. It is observed that as Q, D_a, R_n, α_0 and L_b increase (see Figs. 10a, 10c, 10d, 10g and 10h), the values of $Nu(t)$ show slightly incremented, thus showing an increase in the heat transport, which are the similar results obtained by Agarwal et al. [44].

According to Figs. 10b, 10e, and 10f, when porosity ε, bioconvection Rayleigh-Darcy number R_b, and modified gyrotaxis number PeG increase, the $Nu(t)$ decreases, indicating a delay in heat transfers.

Figs. 11a-11d and 12a-12d depict the temporary behavior of Sherwood number $Sh(t)$, for varying values of magnetic field (Chandrasekhar number Q), porosity ε, Darcy number D_a, nanoparticle concentration Rayleigh-Darcy number R_n, bioconvection Rayleigh-Darcy number R_b, modified gyrotaxis number PeG, geometric shape of microorganisms α_0 and bioconvection Lewis number L_b.

As shown in Figs. 11a-11d and 12a-12d, the stationary level of mass transfer of nanoparticles is reached in less time than heat transfer. The Sherwood number varies at small intervals depending on the parameters $(Q, \varepsilon, D_a, R_n, R_b, PeG, \alpha_0, L_b)$. Because of the basic distribution of the volumetric concentration of nanoparticles (22), the stationary value of the Sherwood number surpasses 1.

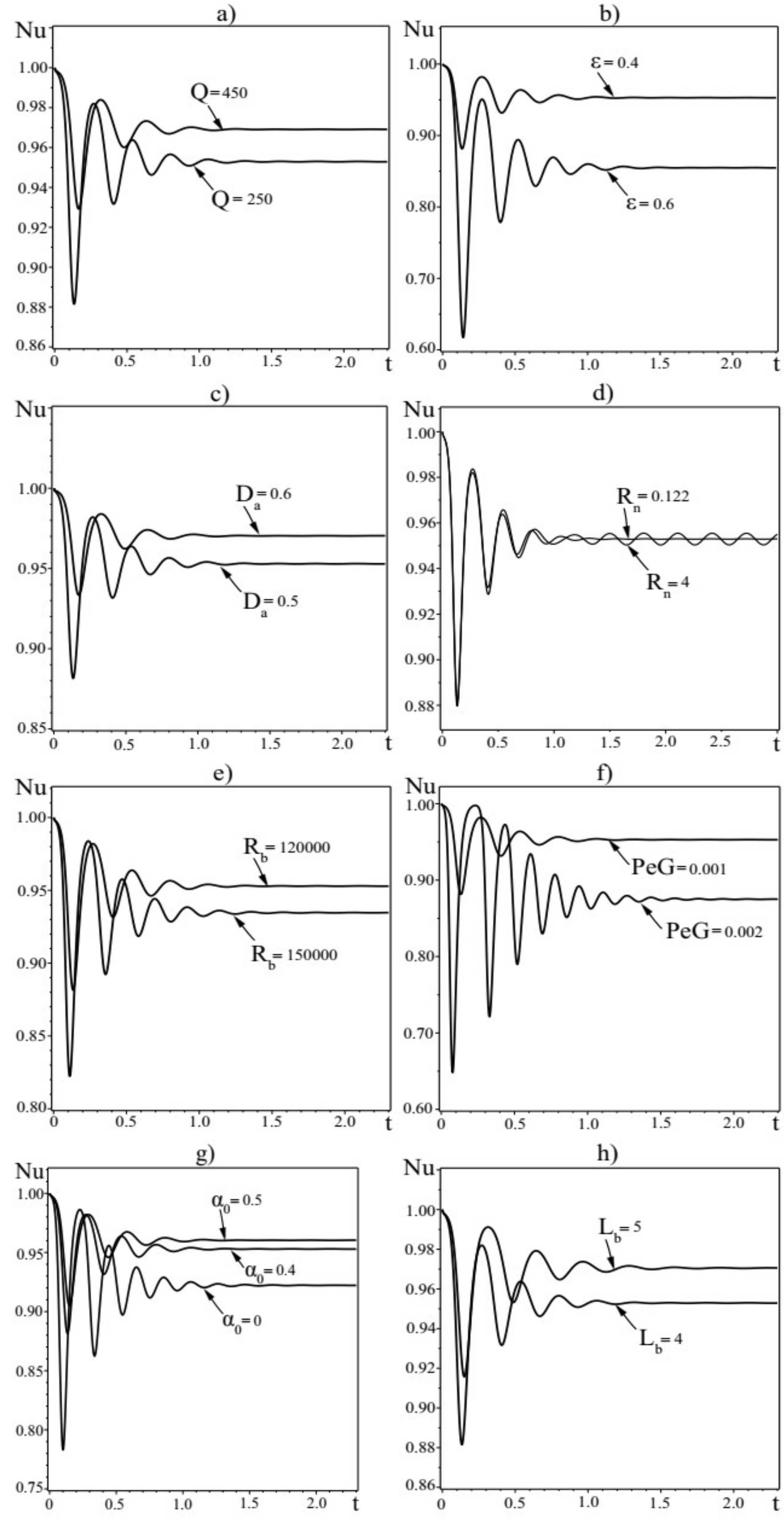

Figure 10. Thermal Nusselt number $Nu(t)$ variation with time t for various values of: a) Chandrasekhar number Q ; b) porosity ε ; c) Darcy number D_a ; d) concentration Rayleigh-Darcy number Ra_n ; e) bioconvection Rayleigh-Darcy number R_b ; f) modified gyrotaxis number PeG ; g) geometric shape of microorganisms α_0 ; h) bioconvection Lewis number L_b .

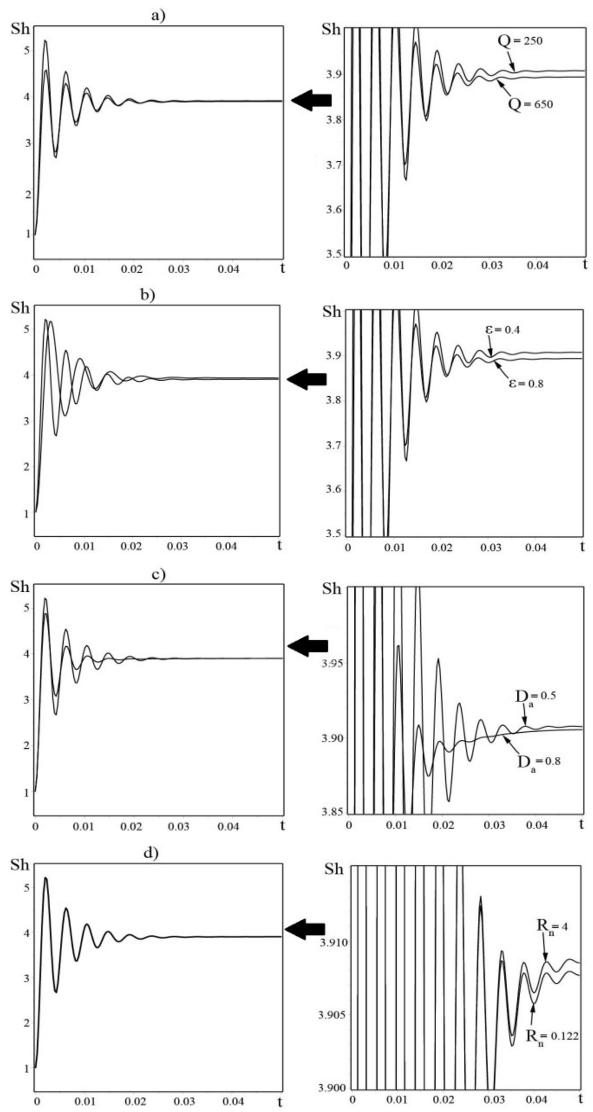

Figure 11. Sherwood number $Sh(t)$ variation with time t for various values of: a) Chandrasekhar number Q ; b) porosity ε ; c) Darcy number D_a ; d) concentration Rayleigh-Darcy number Ra_n .

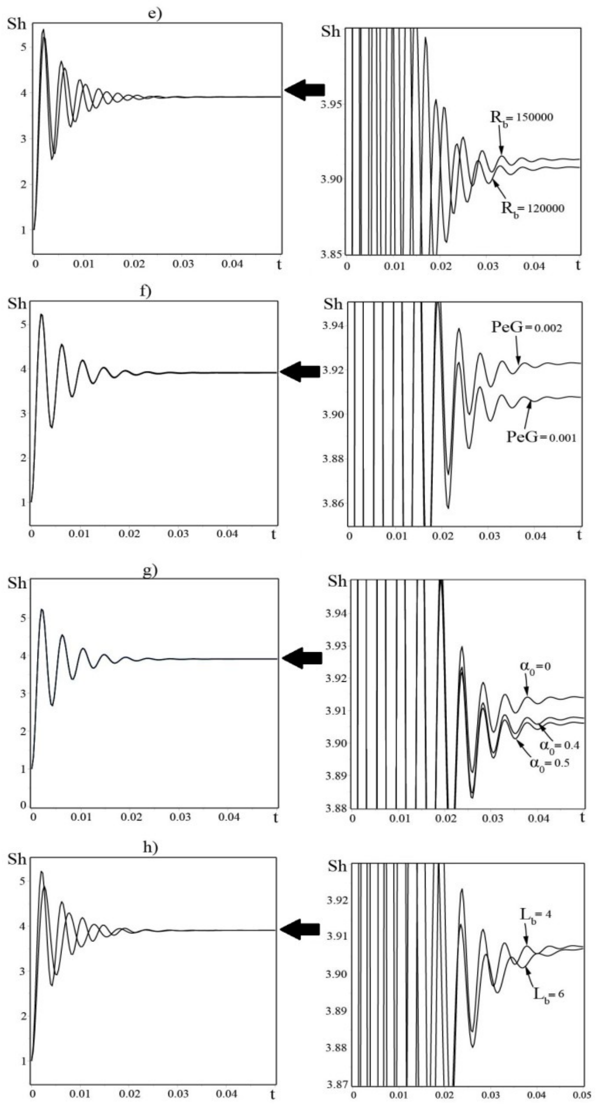

Figure 12. Sherwood number $Sh(t)$ variation with time t for various values of: e) bioconvection Rayleig-Darcy number R_b ; f) modified gyrotaxis number PeG ; g) geometric shape of microorganisms α_0 ; h) bioconvection Lewis number L_b .

8. CONCLUSIONS

Under a vertical magnetic field, we investigated linear stability in a horizontal porous media saturated by nanofluid and gyrotactic microorganisms, heated from below and cooled from above, using the Darcy-Brinkman model, which incorporates Brownian motion and thermophoresis. The system with nanoparticle distribution at the top of the fluid layer has also been proposed. The influence of gyrotaxes on the orientation of swimming microorganisms was used in this study. The normal mode method was used for the linear analysis. The impact of various factors on the development of thermal instability was then established. The results are graphically represented. The following are our conclusions for Al_2O_3-water nanofluid with gyrotactic microorganisms:

- The vertical magnetic field and Darcy number enhance the stability of the system.
- Medium porosity, Lewis number, modified diffusivity ratio and concentration Rayleigh number have a destabilizing influence on the stationary convection of the system.
- An increase in the concentration of gyrotactic microorganisms (or modified bioconvection Rayleigh-Darcy number) enhances the onset of magnetic convection.
- Spherical gyrotactic microorganisms contribute more effectively to the development of thermal instability.

Similar conclusions are also valid for metallic and semiconductor nanofluids. It has been determined that copper-nanofluid is more stable than silver-water, whereas silicon oxide-water nanofluid is more stable than titanium oxide-water nanofluid, according to a comparative investigation of thermal instability using metallic and semiconducting nanofluids.

Graphic representation of the nonlinear theory results for Al_2O_3-water nanofluid containing gyrotactic microorganisms. The following conclusions may be taken from these research results:

- The convective heat transport (Nusselt number $Nu(t)$) is enhanced with increasing Q, D_a, R_n, α_0, and L_b.
- Convective heat transport decreases as ε, R_b, and PeG increase.
- When the parameters $Q, \varepsilon, D_a, R_n, R_b, PeG, \alpha_0$, and L_b are changed, the stationary value of mass transfer is established faster than convective heat transfer and is approximately $Sh(t) \approx 3.9$ at an initial value of $Sh(0) = 1$.

The results of the theoretical studies presented in this work can be applied in geophysics, especially in the study of sea flows through a porous medium (the ocean crust) containing nanoparticles and gyrotactic microorganisms, as well as in designing biosensors.

ORCID IDs
Michael I. Kopp, https://orcid.org/0000-0001-7457-3272; **Volodymyr V. Yanovsky**, https://orcid.org/0000-0003-0461-749X
Ulavathi S. Mahabaleshwar, https://orcid.org/0000-0003-1380-6057

REFERENCES

[1] D. Ingham and L. Pop, *Transport Phenomena in Porous Media* (Elsevier, Oxford, 2005).
[2] D. A. Nield and A. Bejan, *Convection in porous media* (Springer, New York, 2006).
[3] P. Vadasz, ''Instability and convection in rotating porous media: A review," Fluids, **4**, 147 (2019), https://doi.org/10.3390/fluids4030147
[4] S. Choi, "Enhancing thermal conductivity of fluids with nanoparticles," in Development and applications of Non-Newtonian flows, Vol. **66**, edited by D. A. Signier and H. P. Wang (ASME, New York, 1995) pp. 99-105.
[5] J. Buongiorno, "Convective Transport in Nanofluids," J. Heat Trans., **128**, 240 (2005), https://doi.org/10.1115/1.2150834
[6] D. Tzou, "Thermal instability of nanofluids in natural convection," Int. J. Heat Mass Transf., **51**, 2967 (2008), https://doi.org/10.1016/j.ijheatmasstransfer.2007.09.014
[7] D.A. Nield, and A.V. Kuznetsov, "Thermal instability in a porous medium layer saturated by a nanofluid," Int. J. Heat Mass Transfer, **52**, 5796 (2009), https://doi.org/10.1016/j.ijheatmasstransfer.2009.07.023
[8] A.V. Kuznetsov, and D A. Nield, "Thermal instability in a porous medium layer saturated by a nanofluid: Brinkman model," Transp. Porous Media, **81**, 409 (2010), https://doi.org/10.1007/s11242-009-9413-2
[9] B.S. Bhadauria, and S. Agarwal, "Natural convection in a nanofluid saturated rotating porous layer: A nonlinear study," Transp. Porous Media, **87**, 585 (2011), https://doi.org/10.1007/s11242-010-9702-9
[10] D. Yadav, G.S. Agrawal, and R. Bhargava, "Thermal instability of rotating nanofluid layer," Int. J. Eng. Sci., **49**, 1171-1184 (2011), https://doi.org/10.1016/j.ijengsci.2011.07.00
[11] G.C. Rana, and R. Chand, "On the onset of thermal convection in a rotating nanofluid layer saturating a Darcy-Brinkman porous medium: a more realistic model," J. Porous Media, **18**, 629 (2015), https://doi.org/10.1615/JPorMedia.v18.i6.60
[12] U. Gupta, J. Ahuja, and R.K. Wanchoo, "Magneto convection in a nanofluid layer," Int. J. Heat Mass Transfer, **64**, 1163 (2013), https://doi.org/10.1016/j.ijheatmasstransfer.2013.05.035
[13] J. Ahuja, U. Gupta, and R.K. Wanchoo, "Hydromagnetic Stability of Metallic Nanofluids (Cu-Water and Ag-Water) Using Darcy-Brinkman Model," Int. J. Geophys., **2016**, 9 (2016), https://doi.org/10.1155/2016/5864203
[14] J. Sharma, U. Gupta, and R.K. Wanchoo, "Magneto Binary Nanofluid Convection in Porous Medium," Int. J. Chem. Eng., **2016**, 8 (2016), https://doi.org/10.1155/2016/9424036
[15] D. Yadav, R.A. Mohamed, H.H. Cho, and J. Lee, "Effect of Hall Current on the Onset of MHD Convection in a Porous Medium Layer Saturated by a Nanofluid," J. App. Fluid Mech., **9**, 2379 (2016), https://doi.org/10.18869/acadpub.jafm.68.236.25048
[16] J. Ahuja, and U. Gupta, "Magneto convection of rotating nanofluids in porous medium: metals and semiconductors as nanoparticles," Research Journal of Science and Technology, **09**, 135 (2017), https://doi.org/10.5958/2349-2988.2017.00022.5
[17] A.J. Chamkha, S.K. Jena, and S.K. Mahapatra, "MHD convection of nanofluids: A review," J. Nanofluids, **4**, 271 (2015), https://doi.org/10.1166/jon.2015.1166
[18] J. Ahuja, and J. Sharma, "Rayleigh-benard instability in nanofluids: a comprehensive review," Micro and Nano Syst. Lett. **8**, 21 (2020), https://doi.org/10.1186/s40486-020-00123-y
[19] T.J. Pedley, N.A. Hill, and J.O. Kessler, "The growth of bioconvection patterns in a uniform suspension of gyrotactic microorganisms," J. Fluid Mech., **195**, 223 (1988). https://doi.org/10.1017/S0022112088002393
[20] N.A. Hill, T.J. Pedley, and J.O. Kessler, "Growth of bioconvection patterns in a suspension of gyrotactic microorganisms in a layer of finite depth," J. Fluid Mech. **208**, 509 (1989), https://doi.org/10.1017/s0022112088002393
[21] T.J. Pedley, and J.O. Kessler, "Hydrodynamic phenomena in suspensions of swimming microorganisms," Ann. Rev. Fluid Mech. **24**, 313 (1992), https://doi.org/10.1146/ANNUREV.FL.24.010192.001525
[22] A.A. Avramenko, "Model of Lorenz instability for bioconvection", Dopov. Nac. akad. nauk Ukr. **10**, 68 (2010).
[23] E. Lorenz, "Deterministic nonperiodic flow," J. Atmos. Sci. **20**, 130 (1963), https://doi.org/10.1175/1520-0469(1963)020<0130:DNF>2.0.CO;2
[24] A.V. Kuznetsov, "The onset of nanofluid bioconvection in a suspension containing both nanoparticles and gyrotactic microorganisms," Int. Commun. Heat Mass Transfer, **37**, 1421 (2010), https://doi.org/10.1016/j.icheatmasstransfer.2010.08.015
[25] A.V. Kuznetsov, "Non-oscillatory and oscillatory nanofluid bio-thermal convection in a horizontal layer of finite depth," Eur. J. Mech. B. Fluids, **30**, 156 (2011), https://doi.org/10.1016/j.euromechflu.2010.10.007
[26] S. Saini, and Y.D. Sharma, "A Bio-Thermal Convection in WaterBased Nanofluid Containing Gyrotactic Microorganisms: Effect of Vertical Throughflow," J. Appl. Fluid Mech., **11**, 895 (2018), https://doi.org/10.29252/jafm.11.04.28062
[27] N. Faiza, A. Shafiq, L. Zhao, and A. Naseem, "MHD biconvective flow of Powell Eyring nanofluid over stretched surface," AIP Advances, 7, 065013 (2017), https://doi.org/10.1063/1.4983014

[28] S. Zuhra, N.S. Khan, Z. Shah, and S. Islam, "Simulation of bioconvection in the suspension of second grade nanofluid containing nanoparticles and gyrotactic microorganisms," Aip Advances, **8,** 105210 (2018), https://doi.org/10.1063/1.5054679
[29] S.M. Atif, S. Hussain, and M. Sagheer, "Magnetohydrodynamic stratified bioconvective flow of micropolar nanofluid due to gyrotactic microorganisms," Aip Advances, **9**, 025208 (2019), https://doi.org/10.1063/1.5085742
[30] A.A.M. Arafa, Z.Z. Rashed, and S.E. Ahmed, "Radiative MHD bioconvective nanofluid flow due to gyrotactic microorganisms using AtanganaBaleanu Caputo fractional derivative," Phys. Scr. **96**, 055211 (2021). https://doi.org/10.1088/1402-4896/abe82d
[31] M.I. Asjad, N. Sarwar, B. Ali, S. Hussain, T. Sitthiwirattha, and J. Reunsumrit, "Impact of Bioconvection and Chemical Reaction on MHD Nanofluid Flow Due to Exponential Stretching Sheet," Symmetry, **13**, 2334 (2021). https://doi.org/10.3390/sym13122334
[32] A.V. Kuznetsov, and A.A. Avramenko, "Stability Analysis of Bioconvection of Gyrotactic Motile Microorganisms in a Fluid Saturated Porous Medium," Transp. Porous Media, **53**, 95 (2003). https://doi.org/10.1023/A:1023582001592
[33] D.A. Nield, A.V. Kuznetsov, and A.A. Avramenko, "The onset of bioconvection in a horizontal porous-medium layer", Transp. Porous Media, **54**, 335 (2004). https://doi.org/10.1023/B:TIPM.0000003662.31212.5b
[34] A.A. Avramenko, and A.V. Kuznetsov, "The Onset of Convection in a Suspension of Gyrotactic Microorganisms in Superimposed Fluid and Porous Layers: Effect of Vertical Throughflow", Transp. Porous Media, **65**, 159 (2006), https://doi.org/10.1007/s11242-005-6086-3
[35] A.V. Kuznetsov, "The onset of thermo-bioconvection in a shallow fluid saturated porous layer heated from below in a suspension of oxytactic microorganisms," Eur. J. Mech. B/Fluids, **25**, 223 (2006), https://doi.org/10.1016/j.euromechflu.2005.06.003
[36] D.A. Nield, and A.V. Kuznetsov, "The cheng-minkowycz problem for natural convective boundary layer flow in a porous medium saturated by a nanofluid: A revised model," Int. J. Heat Mass Transfer, **65**, 682 (2013), https://doi.org/10.1016/j.ijheatmasstransfer.2013.06.054
[37] M. Zhao, S. Wang, H. Wang, and U.S. Mahabaleshwar, "Darcy-Brinkman bio-thermal convection in a suspension of gyrotactic microorganisms in a porous medium", Neural Comput. Appl, **31**, 1061 (2019), https://doi.org/10.1007/s00521-017-3137-y
[38] A. Mahdy, "Gyrotactic Microorganisms Mixed Convection Nanofluid Flow along an Isothermal Vertical Wedge in Porous Media", Int. J. Aerosp. Mech. Eng. **11**, 840 (2017). https://doi.org/10.5281/zenodo.1130959
[39] A. Alsenafi, and M. Ferdow, "Dual solution for double-diffusive mixed convection opposing flow through a vertical cylinder saturated in a darcy porous media containing gyrotactic microorganisms", Sci. Rep., **11**, 19918 (2021), https://doi.org/10.1038/s41598-021-99277-x
[40] H.A. Nabwey, S.M.M. EL-Kabeir, A. Rashad, and M. Abdou, "Gyrotactic microorganisms mixed convection flow of nanofluid over a vertically surfaced saturated porous media", Alex. Eng. J. **61**, 1804 (2022), https://doi.org/10.1016/j.aej.2021.06.080
[41] S. Chandrasekhar, *Hydrodynamic and Hydromagnetic Stability* (Dover, New York, 1981).
[42] Y. Yang, Z.G. Zhang, E.A. Grulke, W.B. Anderson, and G. Wu, "Heat transfer properties of nanoparticle-in-fluid dispersions (nanofluids) in laminar flow," Int. J. Heat Mass Transfer, **48**, 1107 (2005), https://doi.org/10.1016/j.ijheatmasstransfer.2004.09.038
[43] J.C. Umavathi, D. Yadav, and M.B. Mohite, "Linear and nonlinear stability analyses of double-diffusive convection in a porous medium layer saturated in a maxwell nanofluid with variable viscosity and conductivity", Elixir Mech. Engg. **79**, 30407 (2015)
[44] S. Agarwal, N. Sacheti, P. Chandran, B.S. Bhadauria, and A.K. Singh, "Non-linear Convective Transport in a Binary Nanofluid Saturated Porous Layer", Transp. Porous Med. **93**, 29 (2012), https://doi.org/10.1007/s11242-012-9942-y
[45] M. Zhao, S. Wang, S. Li, Q. Zhang, and U. Mahabaleshwar, "Chaotic Darcy-Brinkman convection in a fluid saturated porous layer subjected to gravity modulation", Results Phys. **9**, 1468 (2018), https://doi.org/10.1016/j.rinp.2018.04.047

БІОТЕРМАЛЬНА КОНВЕКЦІЯ В ПОРИСТОМУ СЕРЕДОВИЩІ, ЯКЕ НАСИЧЕНЕ НАНОРІДИНОЮ ТА МІСТИТЬ ГІРОТАКТИЧНІ МІКРООРГАНІЗМИ, ПІД ЗОВНІШНІМ МАГНІТНИМ ПОЛЕМ

Михайло Й. Копп[a], Володимир В. Яновський[a,b], Улаваті С. Махабалешвар[c]
[a]*Інститут монокристалів, Національна Академія Наук України*
пр. Науки 60, 61001 Харків, Україна
[b]*Харківський національний університет імені В.Н. Каразіна*
майдан Свободи, 4, 61022, Харків, Україна
[c]*Факультет математики, Шіваганготрі, Університет Давангере, Давангере, Індія 577 007*

Вивчення теплової конвекції в пористих середовищах, які насичені нанорідиною та мікроорганізмами, є важливим завданням для багатьох геофізичних та інженерних програм. Концепція суміші нанорідин та мікроорганізмів приваблює багатьох дослідників через її здатність покращувати теплові властивості та, як наслідок, швидкості теплообміну. Ця властивість активно використовується як в електронних системах охолодження, так і біофізиці. Таким чином, метою цього дослідження є вивчення біотермальної нестійкості в пористому середовищі, яке насичене нанорідиною на водній основі, що містить гіротактичні мікроорганізми, у присутності вертикального магнітного поля. Наявність зовнішнього магнітного поля як у природних, так і в технологічних ситуаціях, стимулювала нас у проведенні цього теоретичного дослідження. З використанням моделі Дарсі-Брінкмана розглянуто лінійний аналіз конвективної нестійкості для обох вільних меж з урахуванням ефектів броунівської дифузії та термофорезу. Для проведення цього аналітичного дослідження було використано метод Галеркіна. Встановлено, що теплообмін здійснюється стаціонарною конвекцією без коливальних рухів. У стаціонарних режимах конвекції аналізуються нанорідини оксидів металів (Al_2O_3), металеві нанорідини (Cu, Ag) та напівпровідникові нанорідини (TiO_2, SiO_2). Збільшення чисел Чандрасекара та Дарсі значно покращує стабільність системи, але збільшення пористості та модифікованого біоконвекційного числа Релея-Дарсі прискорюють початок нестійкості. Для визначення перехідного режиму тепломасоперенесення застосовується нелінійна теорія, заснована на представленні методу рядів Фур'є. На малих проміжках часу числа Нуссельта та Шервуда мають коливальний характер. Числа Шервуда (масообмін) у часовому інтервалі досягають стаціонарних значень швидше, ніж числа Нуссельта (теплообмін). Це дослідження може допомогти у вивченні конвекції морської води в океанічній корі, а також у створенні біосенсорів.

Ключові слова: нанорідина, біотеплова конвекція, сила Лоренца, термофорез, броунівський рух, гіротактичний мікроорганізм, магнітне поле